# ZECHSTEIN SALT DENMARK
# Salt Research Project EFP-81

## Volume IV
## Microthermometry

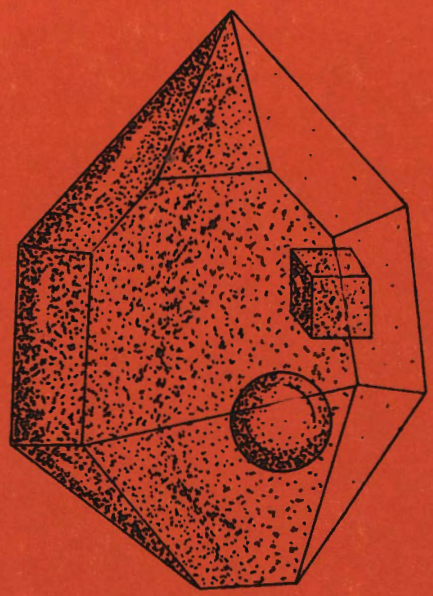

DGU
Geological Survey of Denmark
1984

# ZECHSTEIN SALT DENMARK
# Salt Research Project EFP-81

Volume IV
Microthermometry

By Johannes Fabricius

July 1984
DGU-report series C no. 1 · 1984

ISBN 87 88640 08 6 (bd. 1-4)

DGU
Geological Survey of Denmark

# PREFACE

Volume IV is part of four volumes elaborated in the course of Salt Research Project EFP-81.

The volume deals with studies of fluid inclusions in halite and quartz crystals from Danish salt domes.

CONTENTS

CHAPTER 1

# STUDIES OF FLUID INCLUSIONS IN HALITE AND EUHEDRAL QUARTZ CRYSTALS FROM SALT DOMES IN THE NORWEGIAN-DANISH BASIN

By Johs. Fabricius

(Sixth International Symposium on Salt. In press.)

CONTENTS

STUDIES OF FLUID INCLUSIONS IN HALITE AND EUHEDRAL QUARTZ CRYSTALS FROM SALT DOMES IN THE NORWEGIAN-DANISH BASIN.


## ABSTRACT

Microthermometric studies have been carried out on fluid inclusions in halite and in euhedral quartz from salt domes in the dome area of N.Jutland, which is a part of the Norwegian-Danish Basin. The investigated salt is of Zechstein age.

Euhedral quartz crystals have been extracted from selected core material from wells in different domes at various depths from 200 m to 3485 m. The homogenization temperature and the melting temperature of the ice and the different hydrates have been measured on fluid inclusions in the quartz crystals. The salinity and the Ca:Mg ratio have been determined from the various phase diagrams of the system $CaCl_2$-$MgCl_2$-NaCl-$H_2O$. Salinity 30 - 40 weight% brine. Ca:Mg ratio: 3:1 - 1:4.

In a few cases both the trapping and the homogenization temperature were measured and the prevailing pressures during the crystallization of the quartz have been calculate. The maximum P and T values may indicate thermal convection in the salt pillow this causing the initiation of the diapiric penetration phase.

A parallel study of fluid inclusions in the corresponding halite has shown, that the physical and the chemical conditions of halite in connection with the brine give rise to inaccurate temperature measurements and too low salinity determinations.

Several workers have studied fluid inclusions in bedded salt, e.g., Dreyer et al., (1949); Roedder, (1963); Powers et al., ed., (1978); Roedder & Belkin, (1979a). To the best of the author´s knowledge only Roedder & Belkin, (1979b), have performed a study of dome salt.

It is obvious from these studies that P-T-X results are ambiguous. For this reason the present study is focused on the fluid inclusions occurring in the small euhedral quartz crystals found in the rock salt. The P-T-X data obtained form these crystals are compared with data from the fluid inclusions in the halite and the genesis of the rock salt and the quartz crystals will be discussed.

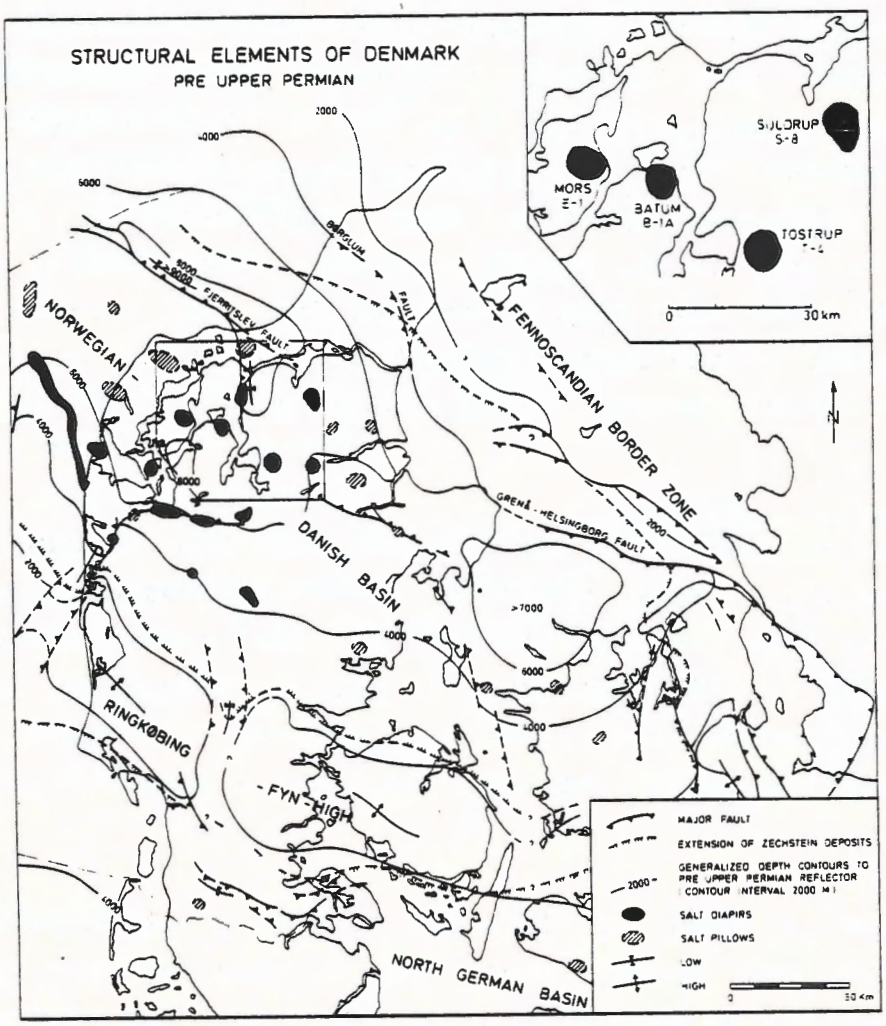


Fig. 1. Map of the halokinesis area in Northern Jutland, Denmark. After Michelsen et al. (1981)

Figure 1 shows the dome area in N.Jutland and the insert map shows the sites, names of the domes and wells mentioned in this paper.

## GEOLOGICAL SETTING

In the Norwegian-Danish Basin (figure 1) evaporites were precipitated during Zechstein time in three main cycles, which are believed to correspond to the North German Zechstein 1, 2 and 3 cycles, Richter-Bernburg, (1960).

The stratigraphy of the Danish Zechstein evaporites is given in table 1 and figure 6. All the thicknesses mentioned are approximate because they originate from wells in strongly deformed sequences within domes. From geophysical evidence it is believed that the diapirism (the pillow phase) was initiated in Late Triassic. The penetration phase is regarded to be Middle Jurassic - Early Cretaceous age and the postdiapiric phase commenced in Late Cretaceous, Richter-Bernburg, (1981).

| Cycle | Symbol | Depth, m | Lithology |
|---|---|---|---|
| Z3 | Na3 | 100-200 | rocksalt, red to brownish to greyish, coarse crystlline, with disseminated anhydrite and two thin zones of potassium and one thin bed of anhydrite. |
| | T3 | 60 | "saltclay", consolidated sandstone, siltstone, claystone, red and green colours, with rocksalt. |
| Z2 | Na2r | 15 | "deckrocksalt", yellowish red to orange red, kieseritic, potassic with clay and anhydrite. |
| | K2 | 10 | hardsalt, kieserite, halite, carnallite, sylvite and clay. (Veggerby K-zone corresponding with Kaliflöz Stassfurt) |
| | Na2(K) | 20 | rocksalt, reddish to brownish red, potassic and kieseritic. |
| | Na2 | 500 | rocksalt, light to medium grey, occ. colourless, coarse crystalline with disseminated small crystals of anhydrite. |
| | Ca2 | 9 | anhydrite-dolomite, alternating layers of anhydrite, dolomite and limestone, medium grey. |
| Z1 | A1 | 1 | anhydrite, brownish, compact. |
| | Na1 | 500 | rocksalt, light to medium grey, occ. colourless, coarse crystalline with disseminated small crystals of anhydrite. |

Table 1. The Stratigraphy of the Danish Zechstein.

In the fluid inclusion study an Olympus petrographic microscope BHA with 10x, 20x and 40x LWD objectives was used in connection with a CHAIXMECA microthermometry apparatus, 1980 model. The heating-freezing stage is commanded by an electronic manual/automatic controller and temperature read-out.

The rocksalt test samples were prepared from cleavage pieces of large colourless halite crystals from selected cores of the Mors El well. The pieces were double polished and had the dimensions of appr. 1x4x4 mm.

The quartz crystals and other water insoluble minerals were separated from 500 g of core material by dissolving the salt in hot water. This residue, containing more than 99% anhydrite, was then separated by heavy liquids and the quartz crystals were eventually separated manually. The quartz crystals were counted and measured and their crystal type was established.

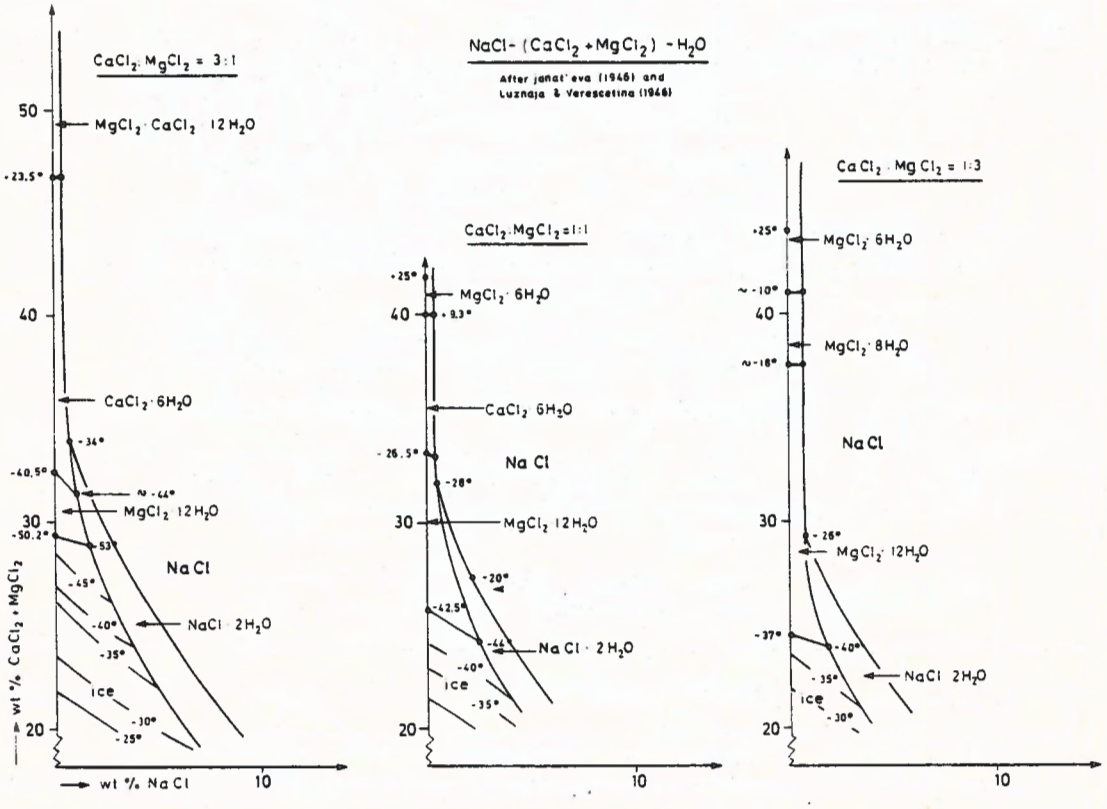


Fig. 2. Phase diagrams in the system NaCl-($CaCl_2$+$MgCl_2$)-$H_2O$, the Ca:Mg ratio 3:1, 1:1, 1:3.

The normal procedure of freezing followed by heating was performed upon the fluid inclusions in the quartz crystals. This procedure is unsuitable in halite as the inclusions leak during the freezing period, therefore the reverse procedure was used.

The salinity and the Ca:Mg ratio of the inclusion fluids were estimated by combining the phase diagrams $CaCl_2$-$MgCl_2$-$H_2O$ and NaCl-$CaCl_2$-$H_2O$, Janat´eva, (1946) and NaCl-$MgCl_2$-$H_2O$ and the three diagrams ($CaCl_2$+$MgCl_2$)-NaCl-$H_2O$, Ca:Mg ratio 3:1, 1:1, 1:3 (fig. 2), Luznaja & Verescetina, (1946).

## FLUID INCLUSIONS IN HALITE

### The inclusions

The fluid inclusions used are believed to be primary, because they are either isolated or form short trains of a few small inclusions, Roedder, (1976, 1979). The great majority of the inclusions are negative cubes with edge lengths averaging 10-12 µm. Small cubes are abundant and cubes with edge lengths of more than 50 µm are rare.

Normally even the smallest inclusions contain one or more crystals of anhydrite, which is not a daughter mineral or a pseudomorph after gypsum. Irregular large inclusions are always found in connection with clusters or tight rows of anhydrite crystals.

After freezing many of the inclusions have developed plane joints parallel to the walls of the inclusions due to the formation of ice and the different hydrates. The joints are filled with very small fluid inclusions during the heating period presumably by diffusion, Gerlach & Heller, (1966) or the liquid is forced out in the joints when heated above the homogenization temperature.

## Thermometry

Especially several of the smaller inclusions have not nucleated a gas phase at room temperature because of a certain metastability, "stretched" fluid Roedder, (1963). A slight cooling to -15° C - 20° C invalidates this metastability and a gas phase is formed. The solubility of NaCl in $CaCl_2$-$MgCl_2$ solution increases with rising temperature, Stewart & Potter, (1979); Jenks, (1979). Due to this it is of importance, that the inclusion has sufficient time to dissolve NaCl from the walls during the heating period and the temperature should therefore be hold close to the homogenization temperature $T_h$.

If the inclusion homogenizes in the fluid phase, i.e., the gas bubble disappears, and the inclusion is heated beyond $T_h$, the pressure in the inclusion increases with ab. 11 bars per C above $T_h$ valid for a 30 weight % NaCl solution, Potter, (1977). The inclusion expands if it does not decrepitate, resulting in a higher $T_h$. An "annealing" of the inclusion has ocurred, Roedder & Belkin, (1979 b). As far as possible the lowermost homogenization temperature should be measured first.

The homogenization temperatures have been measured in the following two intervals:

28.5 °C - 124.8°C, n=68, mean Th= 72.6°C +/- 5.9°C.
189.8 °C - 223.2°C, n=23, mean Th=203.2°C +/- 2.5°C.

Some few inclusions showed $T_h$ above 300°C obviously due to stretching.

## Cryometry

In order to measure the freezing-point depression, and hence determine the chemistry of the fluids, the inclusions were cooled down to -90°C - -110°C. By a slow

rise of the temperature the majority of the inclusions nucleated ice and hydrate at a later stage. The formation of ice was often spontaneous, sometimes arising from a single nucleus.

The melting point of the ice, $T_m$,ice, was measured. This temperature cannot be verified by lowering the temperature until recurring ice formation, because a part of the liberated liquid instantaneously reacts with the walls forming NaCl hydrate. The new $T_m$ ice will then be lower than the first one giving a false, lower freezing-point depression. Since at least three different hydrates are present, of which $NaCl \cdot 2H_2O$ optically is dominatant by a furrowing the inclusion walls, it is impossible as a rule to measure the melting points of $MgCl_2 \cdot 12H_2O$ and especially $CaCl_2 \cdot 6H_2O$. In a few cases the melting point of $MgCl_2 \cdot 12H_2O$ could be measured, because comparatively much liquid was suddenly released.

The melting point of the ice, $T_m$, ice, is measured in the interval -51 °C - -25 °C, n=75, mean $T_m$, ice= -37.6 °C +/- 1.8 °C.

In the following cases $T_m$, ice and the melting point of $MgCl_2 \cdot 12H_2O$ was measured before the $NaCl \cdot 2H_2O$ destroyed the walls:

| $T_m$,ice | $T_m$,hyd. | Salinity min. | Ca:Mg appr. |
|---|---|---|---|
| -40.6°C | -34.6°C | 30 wt% | 1:1 |
| -50.6 | -33.6 | 32 | 2:1 |
| -38.8 | -28.9 | 29 | 1:3 |
| -40.1 | -36.6 | 32 | 1:1 |
| -42.0 | -33.8 | 32 | 1:1 |
| -32.7 | -29.8 | 29 | 1:3 |
| -44.5 | -34.5 | 33 | 2.5:1 |

Table 2.
Salinity and Ca:Mg ratio.

The salinity and the Ca:Mg ratios are determined from the phase diagrams figure 2. The melting point of $CaCl_2 \cdot 6H_2O$ was not measured, hence the true salinity is supposed to be 5-10 wt% higher than the above noted. The NaCl content is less than 2 wt% at 20 °C.

Due to the reasons mentioned above the results of the thermometry and the cryometry are of fair validity only. They can only indicate the conditions in situ.

## Thermometry

In order to find the trapping temperature $T_t$ of the inclusions the homogenization temperatures $T_h$ have to be corrected for the prevailing pressure. For $T_h$ less than 50-60 °C the pressure correction is negligible. An estimate of the pressure prevailing during the formation of inclusions with $T_h$ higher than 60 °C is impossible, because they may have formed at any stage between the bedded salt phase, and the post-diapiric phase or even later.

The homogenization temperatures might only represent an approach to equilibrium volume relations at the pressure and the temperature of the samples site Roedder & Belkin, (1979 b).

In spite of the unacceptable high $T_h$ values it should be noted that they are comparable to the highest values obtained on inclusions in the quartz crystals.

## Cryometry

The amount of supercooling shows, that the fluids are very clean, free from submicroscopic freezing nuclei. This may indicate that clay material may have settled in advance of the halite crystallization.

The fluids in the inclusions may represent seawater, trapped within the original salt, which has coalesced during flow, Roedder & Belkin, (1979 b). In the present work the cryometric results exclude the possibility of any other source than seawater, which is highly concentrated in the halite facies.

## The quartz crystals

Euhedral quartz crystals in saline sediments may have stratigraphical significance in local areas, Shettler, (1972). As the formation of the crystals depends on many factors in saline environments and as the crystals are very sensitive to facial changes, they may be useful as facies indicators, Nachsel, (1966).

The stratigraphical significance is based on the number of crystals (in 500 g of cuttings or core material), their colour, the axis ratio c:a, the crystal habit and the enclosures, Shettler, (1972). Tarr (1929) has set up a growth series from the pseudocubic positive rhombohedron r to the doubly terminated long prismatic form r+z+m. This growth series Grimm, (1962) has named type I-VI (fig. 3) and he suggests an authigenic postsedimentary or early diagenetic formation of the

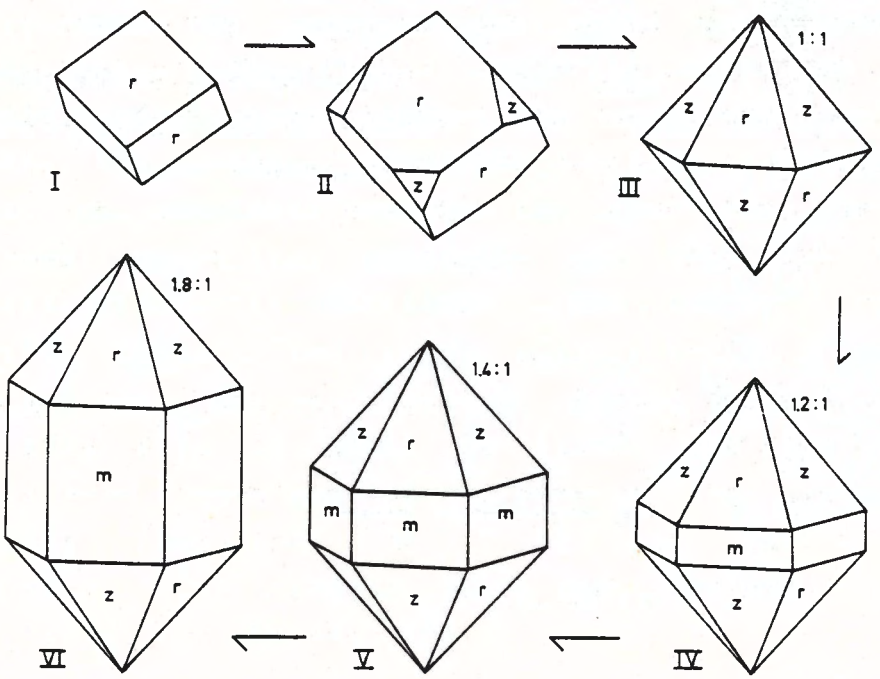


Fig. 3.
The quartz crystal growth series. After Grimm (1962).

crystals. Nachsel, (1966) points out that a synsedimentary origin must be very rare and a silica transport during the saltmetamorphosis seems impossible. Thus he interpreted the crystallization to have taken place during the diagenesis.
The quartz crystals contain a considerable number of anhydrite inclusions, which as a rule are prismatic automorphic microsrystals. This poikilitic structure indicates, that the formation of the quartz crystals began at the same time as incipient anhydrite precipitation, Demangeon, (1966). Demangeon also found that anhydrite precipitation begins when the volume of the seawater is reduced to 1:22.

The present investigation is mainly based on the Batum 1A well (fig. 4), which was drilled in 1951 with continuous coring from the salt mirror at a depth of 206 m to a total depth of 762 m. The core recovery in the uppermost appr. 120 m of the salt was zero. As the salt in the well is

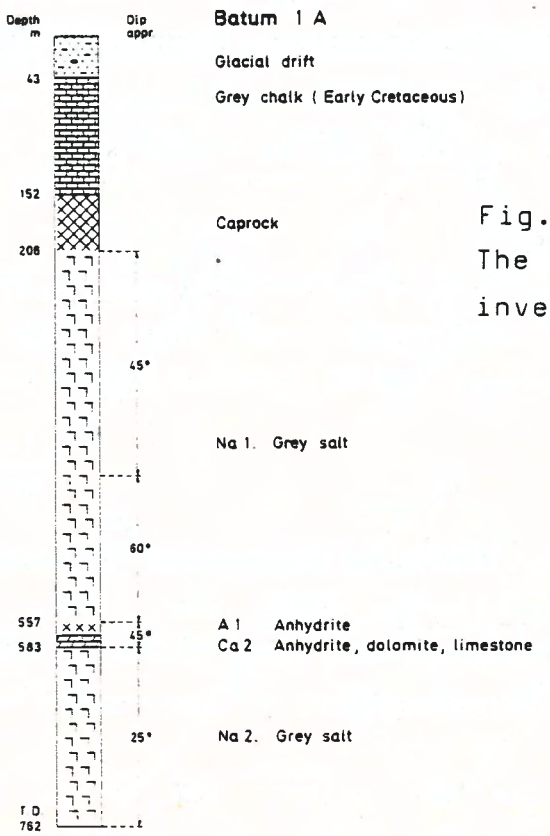


Fig. 4. The Batum 1A well. The Z1 and Z2 layers are inverted.

referred to the Na1 and Na2 salt units, cores from the Mors and the Tostrup domes were selected in such a way that the entire stratigraphic column was represented.

The extracted quartz crystals from the Batum 1A well are all perfect euhedral crystals with sharp edges and smooth crystal faces with practically no lineages or mosaic structures. The habit is of the types III-VI (fig. 3). Generally the r faces are larger than the z ones and on type III crystals one or two m faces may be developed. Some of the crystals are slightly distorted. Intergrown twin crystals with parallel c-axes and with four or three pyramids are common. In this study crystals of type I and II have not been found.

The crystals are colourless and transparent. A few are light yellow to light red with a yellow tint but still transparent. The length of the crystals range from less than 63 µm to 1.4-1.6 mm regardless of the crystal type, and the width of these corresponds with the c:a ratio noted on fig. 3.

The number of the crystals pr 500 g core material ranges from very few up to some few hundreds with an average number of 50-60. None of the types are dominant, though type VI is slightly more abundant than the other types. In relatively few crystals the solid enclosures are poikilitically distributed anhydrite crystals, still regardless of the crystal type. In the majority of the crystals the number of anhydrite crystals is middling to scarce. The anhydrite crystals are larger than the above mentioned poikilitic anhydrite and they are better crystallographically developed. The quartz crystals generally contain one or more clastic grains of quartz, which are small and well rounded. Around these grains a very thin film of brine is found. The film becomes visible when frozen and it splits up into vermicular branching inclusions of fluid and gas at room temperature. The characteristics mentioned are valid for both the Na1 and the Na2 salt.

## The fluid inclusions

Two types of inclusions are found: isolated regular ones (negative crystals) and families of very thin irregular

inclusions situated on an m, r or z crystallographic interface (fig. 5). The irregular inclusions are by far the most common. All the inclusions studied are primary, Roedder, (1976, 1979). Secondary inclusions are extremely rare.

The inclusions usually contain a fluid phase and a gas phase. In very few inclusions also one or two daughter minerals are present (fig. 5). The daughter minerals are halite and also rarely sylvine.


Fig. 5. Irregular thin fluid inclusions containing liquid, gas and a thin "cube" of halite in some of the inclusions. The inclusion family is situated on an m interface appr. 100 µm below the crystal face.

Quartz crystals from other stratigraphic levels

The Na2(K) salt has been sampled from the Mors El well at a drilled depth of 2715 m. The salt, which is potassic and strongly kieseritic (hardsalt), is devoid of quartz crystals.

The potassium zone K2 and the "deck rocksalt" Na2r were studied in the Mors El well from drilled depths of 2800 m and 2883 m. The quartz crystals are all long prismatic (type VI) crystals. The crystal faces are practically all developed with a tight mosaic structure, which rarely allows any microthermometrical measurement. The number of crystals is very large compared to other lithostratigraphical units. The salt T3 of the Tostrup 4

well from a depth of 525 m is correlated with the clay at 2802 m in the E1 well. The correlation is based upon the content and type of quartz crystals, the large number of well developed small pyrite octahedrons and of perfectly developed small brownish rhombohedrons of a carbonate mineral. The quartz crystals are identical with the above mentioned with exception of a red coloured patchy coating on several of the crystals.

The Na3 salt, taken from the Tostrup 4 well at a depth of 1012 m is very deficient in quartz crystals, and these are of the same types as found in the Na1 and Na2 salt. The crystals have not been studied.

## Cryometry on quartz inclusions

None of the inclusions in quartz crystals from K2, Na2r and T3 nucleated ice or hydrate during the freezing procedure, though the temperature was held below -125 °C for long periods.

Many of the inclusions in crystals from Na1 and Na2 acted in the same manner, especially the smaller ones. But some of the larger inclusions with lengths of more than 10 µm nucleated either hydrate alone or ice plus hydrate during the freezing period.

Using the phase diagrams (fig. 2) combined with the other diagrams of Janat´eva, (1946) and Luznaja & Verecetina, (1946) the salinity and the Ca:Mg ratio is determined. As it is known, that the brine under all conditions must be saturated with respect to NaCl, the melting point of $MgCl_2 \cdot 12H_2O$ on the freezing-point depression curve of the phase diagrams (fig. 2) can be used in determining the Ca:Mg ratio. The melting point of $MgCl_2 \cdot 12H_2O$ is established when a lot of brine suddenly is released after melting of the ice, though this does not occcur in all cases. The salinity is determined using the melting point of the $CaCl_2$- hydrate on the freezing-point depression curve, assuming that no

halite crystal is present. If a halite crystal is present, the determination of the true salinity is difficult due to the lack of isotherms in the NaCl-field of the diagrams.
Using the isotherms at the $CaCl_2$-NaCl-$H_2O$ diagram a rather inaccurate estimate of the NaCl content can be established. The results of the cryometry study are shown on figure 6 in the column headed SALINITY.

Thermometry on quartz inclusions

The homogenization temperature $T_h$ corresponds to the disappearence of the gas phase, also if the inclusion contains a solid phase (a daughter mineral) at $T_h$.
Figure 6 illustrates homogenization temperatures of various stratigraphical levels. The mean $T_h$ is indicated by the black triangle and the spread of the $T_h$ values is illustrated.

The two histograms in the column DISTRIB.$T_h$ show the distribution of the homogenization temperatures measured in Zechstein 1 and Zechstein 2 respectively. The mean temperature $T_h$ with 95% confidence limits and the standard deviation are noted.
Five crystals only contain inclusions with halite cubes, which dissolve at a higher temperature $T_t$ than the corresponding $T_h$, see the column CRYSTALLIZATION CONDITIONS. Based upon the difference $T_t - T_h$ the pressure P has been calculated by the method of Potter, (1977).

In order to compare the results obtained on inclusions in halite with the corresponding inclusions in quartz crystals, the crystals were extracted from the rocksalt in question (Mors El.19). Two populations of $T_h$ were observed:

35 °C - 68 °C; Th=51.2 °C +/- 3.5 °C; n=32
70 °C -105 °C; Th=87.8 °C +/- 2.7 °C; n=42

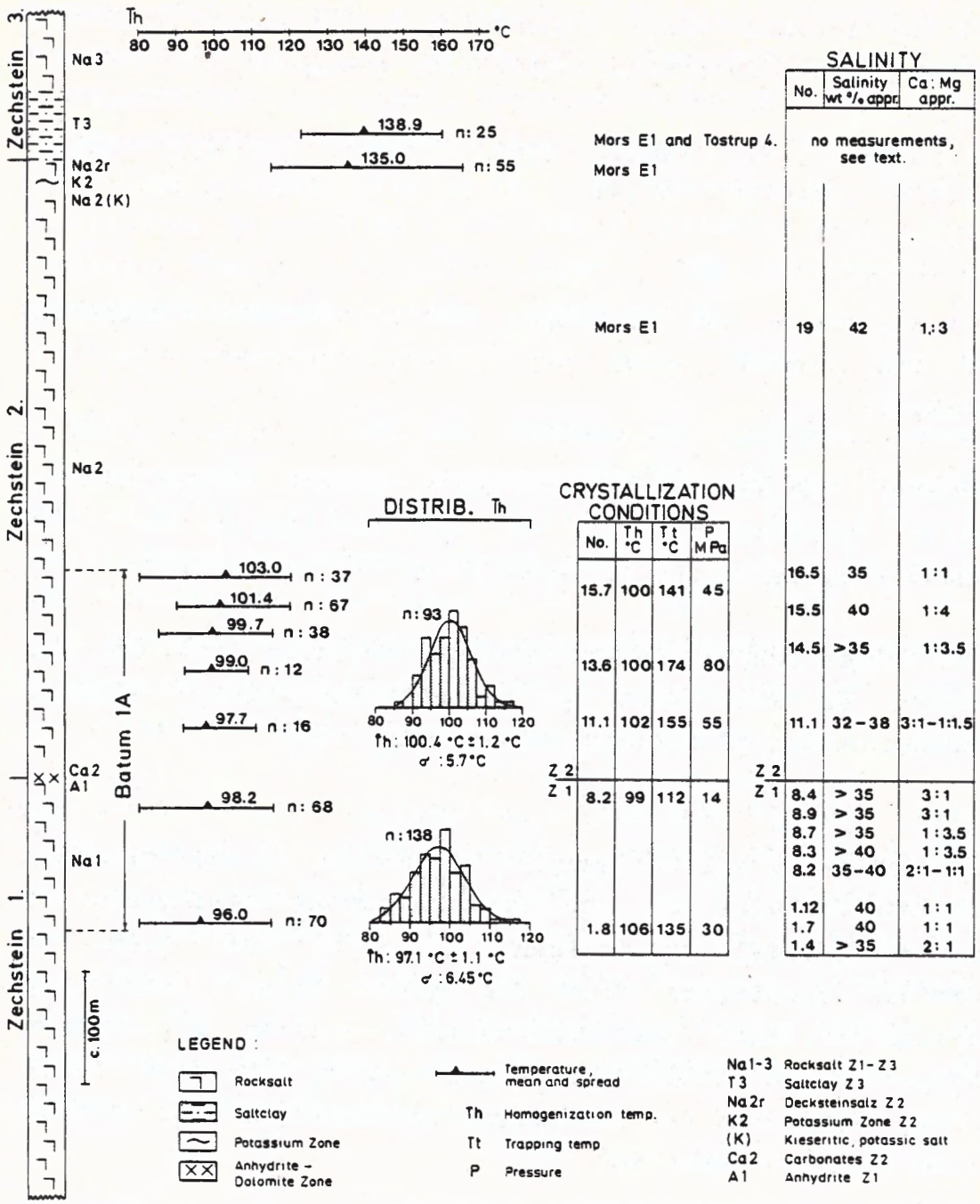


Fig. 6. The three Zechstein evaporite cycles in North Jutland and the results of the microthermometrical study.

## DISCUSSION

In 1948 the Suldrup 8 well was drilled through Na1 salt, A1, Ca2 and Na2 salt. In a depth of 408 m, when the A1 anhydrite was reached, a brine pocket was hit resulting

in an artesic well. According to Dinesen (1961) the brine had the following composition (weight%):

Salinity: 31%; NaCl: 3.95%; KCl: 3.55%; $CaCl_2$: 15.15%; $MgCl_2$: 8.10%; Ca:Mg ratio 1.9:1; pH: 3.18 (20°C).

The salinities and the composition of the brines measured in the present study are in good agreement with this analysis.

However, the Suldrup 8 brine has a higher Ca:Mg ratio, which corresponds fairly well with the samples Nos. 8.4 and 8.9 close to the A1 layer (fig. 6, SALINITY).

The brines trapped in the quartz crystals and in the halite as well must be concentrated seawater with no contamination of foreign brines (fig. 7).

In practially all the samples of Na2 and in the majority of the samples of Na1 from Batum 1A small grains or perfect crystals of authigenic kieserite were found in various quantities from one grain to more than fifty grains/crystals. This observation indicates a seawater concentration within NaCl facies ranging into Mg,K facies (fig. 7). Some few inclusions containing a cube of NaCl also contain a cube KCl.

The solubility of NaCl in a $CaCl_2$,$MgCl_2$ brine increases rather markedly at temperatures above c.100°C, Stewart & Potter, (1979). As the in situ brine, from which the quartz crystals have been precipitated, must be saturated with respect to NaCl, the dissolving temperature $T_s$, higher than $T_h$, of a cube of NaCl present in the inclusion, is the true trapping temperature $T_t$.

Knowing $T_t$ and $T_h$, the pressure prevailing on the brine in situ during the crystallization can be calculated, if the salinity is established. Using the diagrams of

Potter, (1977) and a salinity of 35 wt%, a factor of 1 MPa per °C above $T_h$ is estimated. The mean $T_t$=175 °C corresponding to the pressure P=80 MPa were the crystallization conditions, when the quartz crystal No. 13.6 precipitated (fig. 6). A pressure of 80 MPa corresponds to c.3.5 km consolidated sediments having an average density of 2.3 g/cc. The corresponding geothermal gradient is appr. 20 (m per °C).

In Early Jurassic times the sedimentary sequence above this particular crystal included 600-700 m Z2 and Z3 salt and saltclay (fig. 6) followed by 3500-3800 m consolidated and unconsolidated sand and clay of Triassic and Jurassic age, Michelsen et al., (1981). Due to the high thermal conductivity of salt the geothermal gradient is supposed to be higher in the salt than in the sandy and clayey sediments.

The quartz crystal in question is proposed to have been precipitated in Early Jurassic, outside or indside the salt pillow developed. The crystal is not authigenic, i.e., a synsedimentary or diagenetic crystallization, but was formed 35-45 million years later than the diagenesis of the Na2 salt. The diagenetic stage is assumed to equivalate conditions of low temperature and low pressure, Braitsch, (1971).

The majority of the inclusions studied having $T_h$, higher than c.100 °C contain no cube of NaCl at 20 °C. Keeping in mind that the inclusion brines are saturated with respect to NaCl the above discrepancy can be explained either by a certain metastability, or that the fluid volume is too small to form a visible cube of NaCl. It is interpreted, that the trapping temperature was 110°C - 120°C corresponding to a pressure of 12-13 MPa. This indicates that the quartz of Na1 and Na2 crystallized very late in Zechstein or very early in Triassic times.

The Mors E1.19 crystals having a $T_h$ value in the interval 35 °C-68 °C may be of diagenetic origin and due to this

they are true authigenic crystals. All other crystals studied are crystallized much later than the diagenesis. The $T_h$ interval 28.5 °C-124.8 °C measured on inclusions in the halite coincides with the corresponding intervals measured at the Mors E1.19 quartz crystals.

At figure 6 it is seen that the mean $T_h$ values in Batum 1A increase slightly from Na1 up through Na2. It is believed, that this trend has no stratigraphic significance, because the temperature differences are small and that the temperatures are not pressure corrected. The differences may be due to statistical inadequacy.

The high $T_h$ values measured in Na2r and T3 indicate a late crystallization and the large number of crystals makes it probable that the crystallization took place after the compaction of the saltclay. The porewater (concentrated seawater) of the clay must have been involved in the formation of the quartz crystals. These $T_h$ values are of stratigraphic significance.

The $T_h$, $T_t$ and P values for crystal No. 13.6 (fig. 6) are mean values of six observations. The masimum $T_t$ measured is 179.7 °C, which combined with the corresponding $T_h$=92.3 °C indicate a maximum pressure P=87 MPa. This pressure corresponds with a post-Zechstein overburden of more than 3800 m.

According to Talbot, (1978) and Talbot et al., (1982) these conditions may cause thermal convection in the salt pillow instead of thermal conduction. An estimate of the Rayleigh number R using the parametres mentioned gives a value well above the critical Rc=656 indicating thermal convection. The diapiric penetration phase may have been triggered by these conditions.

The crystal morphologies (fig. 3) probably do not represent a growth series in the salt studied. The reason is that no ghost crystals or thermal zonation

within the crystals have been found. Large type III crystals are found in connection with very small type VI crystals. Twins always consist of the same type as do intergrown crystal aggregates.

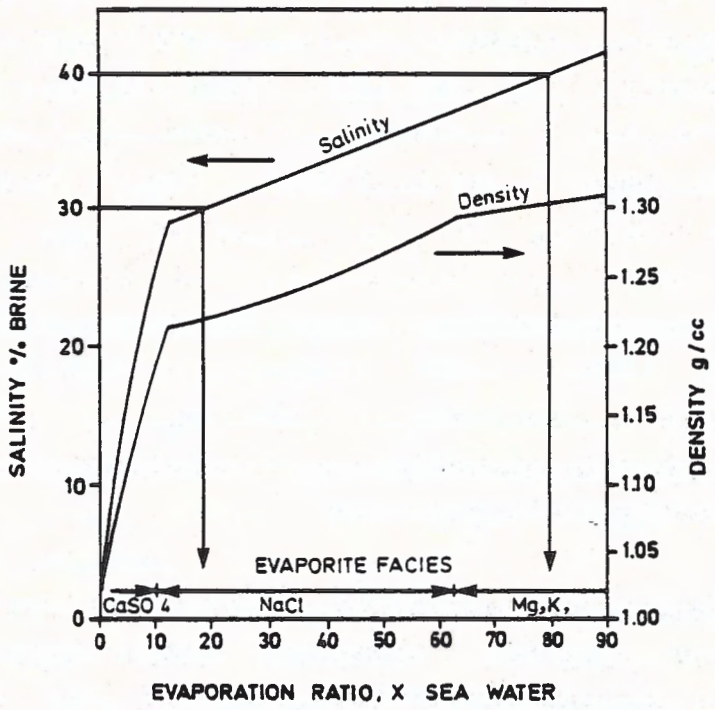


Fig. 7. Density and salinity of concentrated seawater. The approximate limits of salinity, this study, are given. After Holser (1979).

## CONCLUSION

Fluid inclusion studies in halite are impeded by the physical and chemical conditions of halite. The results obtained are fairly inaccurate and they indicate tendencies only.

A few of the quartz crystals studied from Na1 and Na2 are true authigenic crystals crystallized during the diagenesis. The great majority of the crystals from Na1 and Na2 are crystallized during the salt pillow phase ranging up to the beginning of the diapiric penetration phase. The crystals are not authigenic sensu stricto, and they have no stratigraphic significance.

A growth series of the crystals from a pseudocubic type to a long prismatic type is believed not to exist.

The fluid inclusion work performed on the quartz crystals has shown, that the crystallization took place in highly concentrated seawater at temperatures between approximately 75 °C and 180 °C. The salinity ranges from 30 to more than 40 weight% salt composed of $CaCl_2$, $MgCl_2$ and less than 2 weight% NaCl. The Ca:Mg ratio ranges from 3:1 to 1:4.

The mean homogenization temperatures show an increase from the lowest level studied in Zechstein 1 to the highest level studied in Zechstein 2. The obvious stratigraphical significance is believed to be invalid due to statistical inadequacy.

The maximum pressure calculated (87 MPa) in connection with the maximum formation temperature (179.7 °C) indicates thermal convection late in the salt pillow phase. These conditions may have initiated the diapiric penetration phase in Early Jurassic times.

## ACKNOWLEDGMENT

I want to thank my collegues, F. Lyngsie Jacobsen, J. Gutzon Larsen and Gunver Petersen for the interest and discussions of the methods described here. The work was supported from a grant from The Ministry of Energy (EFP 81).

## REFERENCES


Braitsch, O., 1971: Salt Deposits, Their origin and Composition, Springer-Verlag, Berlin, Heidelberg, New York, 297 p.

Demangeon, P., 1966: A propos des quartz authigènes des terrains salifères: Bull. Soc., frans., Miner. Crist., v. 89, p 484-487.

Dinesen, B., 1961: Salt Mineralvand fra Danmarks dybere Undergrund: DGU. IV Række. Bd. 4. Nr. 6., 20 p.

Dreyer, R.M., Garrets, R.M. & Howland, A.L., 1949: Liquid inclusions in halite as a guide to geologic thermometry: Am. Min., v. 34, p 26-34.

Gerlach, H., & Heller, S., 1966: Über Künstliche Flüssigkeitseinschlüsse in Steinsalzkristallen: Ber. Deutsch Ges. Geol. Wiss. B. Miner. Lagerstättenf., v. 11.2, p 195-214.

Grimm, W-D., 1962: Idiomorphe Quarze als Leitmineralien für salinare Fazies: Erdöl und Kohle., v. 11, p 880-887.

Holser, W.T., 1979: Mineralogy of Evaporites: Marine Minerals, Mineralogy Society of America, Short Course Notes, (Burns, R.B. ed.), 380 p.

Janat´eva, O.K., 1946: Polytherms of solubility of salts in the tropic system $CaCl_2$-$MgCl_2$-$H_2O$ and $CaCl_2$-NaCl-$H_2O$: Jour. apl. chem. v. 19, p 709-722 (in Russian).

Jenks, G.H., 1979: Effects of temperature, temperature gradients stress and irradiation on migration of brine inclusions in a Salt repository: ORNL-5526, 73 p.

Luznaja, N.P. & Verescetina, I.P., 1946: Sodium, calcium and magnesium chlorides in aqueous solutions of -57 to +25 (polythermic solubility): Jour. apl. Chem. v. 19, p. 723-733, (in Russian).

Michelsen, O., et al, 1981: Kortlægning af potentielle geotermiske reservoirer i Danmark: Geol. Surv. Denmark. Series B, No. 5, 96 p.

Nachsel, G., 1966: Quarz als Faziesindikator: Zeitschr. amgew. Geol. v. 12, 6, p 322-326.

Potter II, R.W., 1977: Pressure corrections for fluid-inclusion homogenization temperatures based on the volumetric properties of the system NaCl-$H_2O$: Jour. Research U.S. Geol. Survey. v. 5, p 603-607.

Powers, D.W., Lambert, S.J., Shaffer, S-E., Hill, L.R. & Weart, W.D., 1978: Geological characterization report: Waste Isolation Pilot Plant (WIPP) Site, Southeastern New Mexico. Chap. 7.5 p 7.47-7.70.

Richter-Bernburg, G., 1960: Geologischer Bericht über Ergebnis der Bisherigen und Planung der weiteren Exploration auf Kalisalze in Nord-Jütland: Kaliboringerne ved Suldrup 1959-1961, v. 1, 175 p. Rapport, udarbejdet af Egnsudviklingsrådets Boreudvalg. København 1962.

Richter-Bernburg, G., 1981: Geological remarks about the North Jutland salt domes in respect of their suitability for radioactive waste disposal. Unpublished report, ELSAM & ELKRAFT, Denmark.

Roedder, E., 1963: Studies of fluid inclusions II: Freezing data and their interpretation: Econ. Geol. v. 58, No. 2, p 167-211.

Roedder, E., 1976: Fluid-inclusion evidence on the genesis of ores in sedimentary and volcanic rocks: Handbook of strata-bound and stratiform Ore Deposits (Wolf, K.H. ed.). v. 2, p 67-110. Elsevier, Oxford.

Roedder, E., 1979: Fluid-inclusions as samples of ore fluids: Geochemistry of hydrothermal ore deposits. pp 798. John Wiley & Sons.

Roedder, E. & Belkin, H.E., 1979 a: Application of studies of fluid inclusions in Permian Salado Salt, New Mexico, to problems of siting the Waste Isolation Pilot Plant: Scientific Basis for Nuclear Waste Management. v. 1, p 313-321. Plenum Press.

Roedder, E., 1976 b: Fluid-inclusions in salt from the Rayburn and Vacherie domes, Louisiana: U.S. Geological Survey Open File Report 79-1675. 25 p.

Shettler, H., 1972: The stratigraphical significance of idiomorphic quartz crystals in the saline formations of the Weser-Ems area, North-Western Germany: Geology of saline deposits. Proc. Hannover Symp. 1968. Unesco, 1972. Earth Sciences. v. 7, p 111-127.

Stewart, D.B. & Potter II, R.W., 1979: Application of physical chemistry of fluids in rock salt at elevated temperature and pressure to repositories for radioactive waste: Scientific Basis for Nuclear Waste Management v. 1, p 297-311. Plenum Press.

Talbot, C.J., 1978: Halokinesis and thermal convection: Nature v. 273, No, 5665, p 739-741.

Talbot, C.J., Tully, C.P. & Woods, P.J.E., 1982: The structural geology of Boulby (Potash) mine, Cleveland, United Kingdom: Tectonophysics, v. 85, p 167-204.

Tarr, W.A., 1929: Doubly terminated quartz crystals occuring in gypsum: Min. Soc. Am. v. 14, p 19-25.

CHAPTER 2

# FORMATION TEMPERATURE AND CHEMISTRY OF BRINE INCLUSIONS IN EUHEDRAL QUARTZ CRYSTALS FROM PERMIAN SALT IN THE DANISH TROUGH

By Johs. Fabricius

(Bulletin de Mineralogie. Vol. 107,2, 203-216.1984)

CONTENTS

# FORMATION TEMPERATURE AND CHEMISTRY OF BRINE INCLUSIONS IN EUHEDRAL QUARTZ CRYSTALS FROM PERMIAN SALT IN THE DANISH TROUGH.


## ABSTRACT

Classic microthermometry has been carried out on fluid inclusions in euhedral quartz from the Batum saltdome in the dome area of N.Jutland, Denmark. The salt studied is of Zechstein 1 and 2 age. The fluid inclusions are either isolated regular inclusions or populations of irregular thin inclusions on an internal crystal face. The inclusions are either fluid-gas inclusions or inclusions also containing a solid phase of NaCl.

The salinity and the $CaCl_2$:$MgCl_2$ ratio have been measured using phase diagrams of the system ($CaCl_2$+ $MgCl_2$)-NaCl-$H_2O$, the Ca:Mg ratios 3:1, 1:1 and 1:3. The salinity determined is from c.35 weight % to more than 45 weight % and the Ca:Mg ratio from c.3:1 to c.1:4.

The homogenization temperatures of 231 fluid-gas inclusions give a mean T =98.1°C indicating a formation of the quartz crystals late in Zechstein 3. The formation temperatures (c.115 °C-c.180°C) and pressures (c.15 MPa-c.90 MPa) have been measured/calculated on 14 quartz crystals indicating an individual crystallization in the period Early Triassic-Early Jurassic times. The calculated Rayleigh numbers indicate condititon of thermal convection in Late Triassic-Early Jurassic times. Both the Zechstein 1 salt and the Zechstein 2 salt were sedimented under uniform conditions.

## Introduction.

The Danish Zechstein saltdomes are studied in preparation for leaching of caverns applicable for storage of natural gas or compressed air. The feasibility of the domes for nuclear waste storage is studied too. In both cases it is of vital importance to avoid layers of potassium salts in consequence of the high solubility of these salts.

As the Zechstein 2 salt contains a layer of potassium salt and kieseritic "Hartsalz" (=Kieserite-sylvine-halite, Braitsch, 1971) close to the top, this salt is not as expedient as the Zechstein 1 salt. This study therefore has been aiming upon detection of differences between the two salts.

## Geological Setting.

In the Danish subbasin (the Danish Trough) of the Norwegian-Danish basin (figure 1) three cycles of Zechstein evaporites were sedimented. The cycles are named Zechstein 1 (Z1), Z2, and Z3 in accordance with the North German Zechstein cycles (Richter-Bernburg, 1960).

In broad outline the salt succession consists of:

Z3: c.100 m unconsolidated salt clay followed by 100-200 m coloured rocksalt.

Z2: c.500 m grey rocksalt followed by c.50 m Hartsalz, potash zone and coloured rocksalt.

Z1: c.500 m grey rocksalt.

There is a transition zone between Z1 and Z2. The zone consists of a 1 m thick layer of anhydrite (A1) at the very top of Z1 and a 9 m thick layer (Ca 2) of dolomite, limestone and anhydrite at the base of Z2. The

transition zone is a very important marker horizon when present. The layer is competent, hard and brittle, and has been broken up into large flakes "swimming" in the rocksalt.

The grey rocksalt (Z1 and Z2) is coarse crystalline with disseminated small tabular crystals of anhydrite. The average amount of anhydrite is 1-2 weight %.

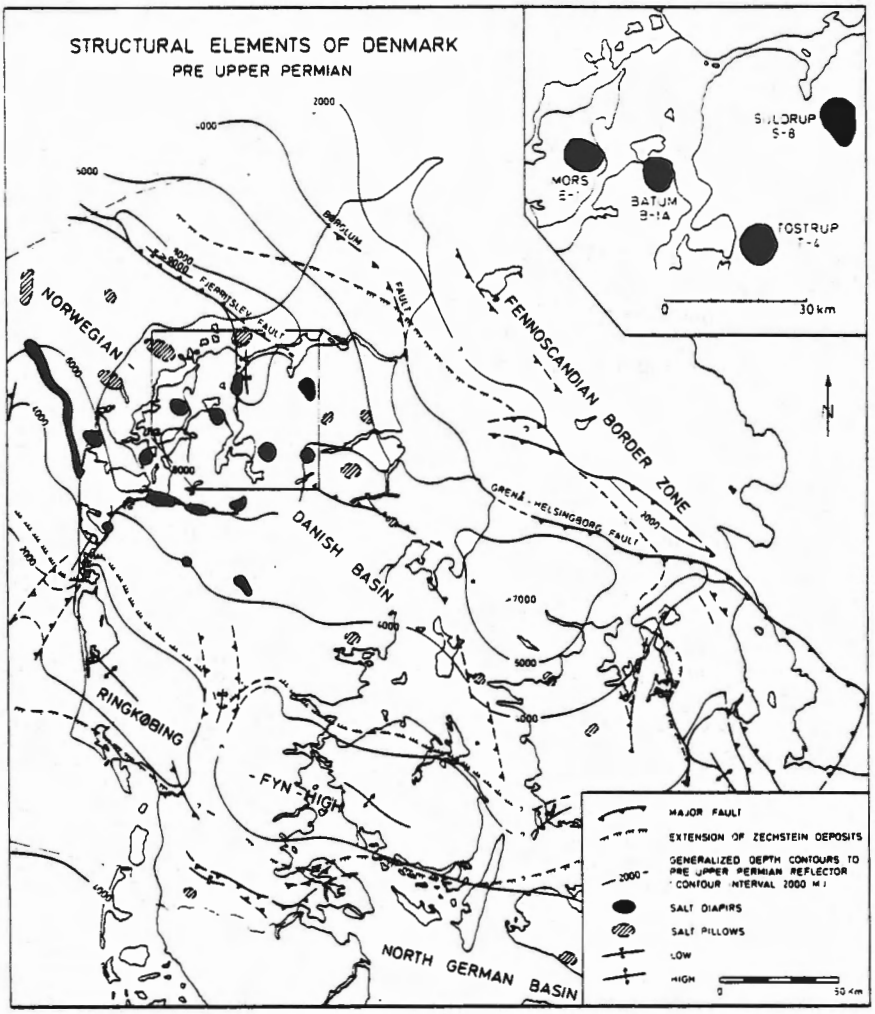


Figure 1. Map of the Zechstein basin with the Batum dome. After Michelsen et al. 1981.

All the thicknesses mentioned are approximate because they were measured in boreholes in strongly deformed sequences within domes. From geophysical evidence it is believed that diapirism (the pillow phase) was initiated in Late Triassic. The penetration phase is regarded as being of Middle Jurassic-Early Cretaceous age and the postdiapiric phase commenced in Late Cretaceous times

(Richter-Bernburg, 1981). The present work has been carried out on well No. 1A drilled in the Batum dome in 1951 (figure 2). During the drilling continuous coring was performed. With the exception of 12 m in the very top of the salt the core recovery of the uppermost c.120 m was zero. The cores were not orientated. Only the dip of the foliation was measured. From figure 2 it can be seen that the layers are inverted, which in connection with the measurements of the dip gives rise to the interpretations drawn.

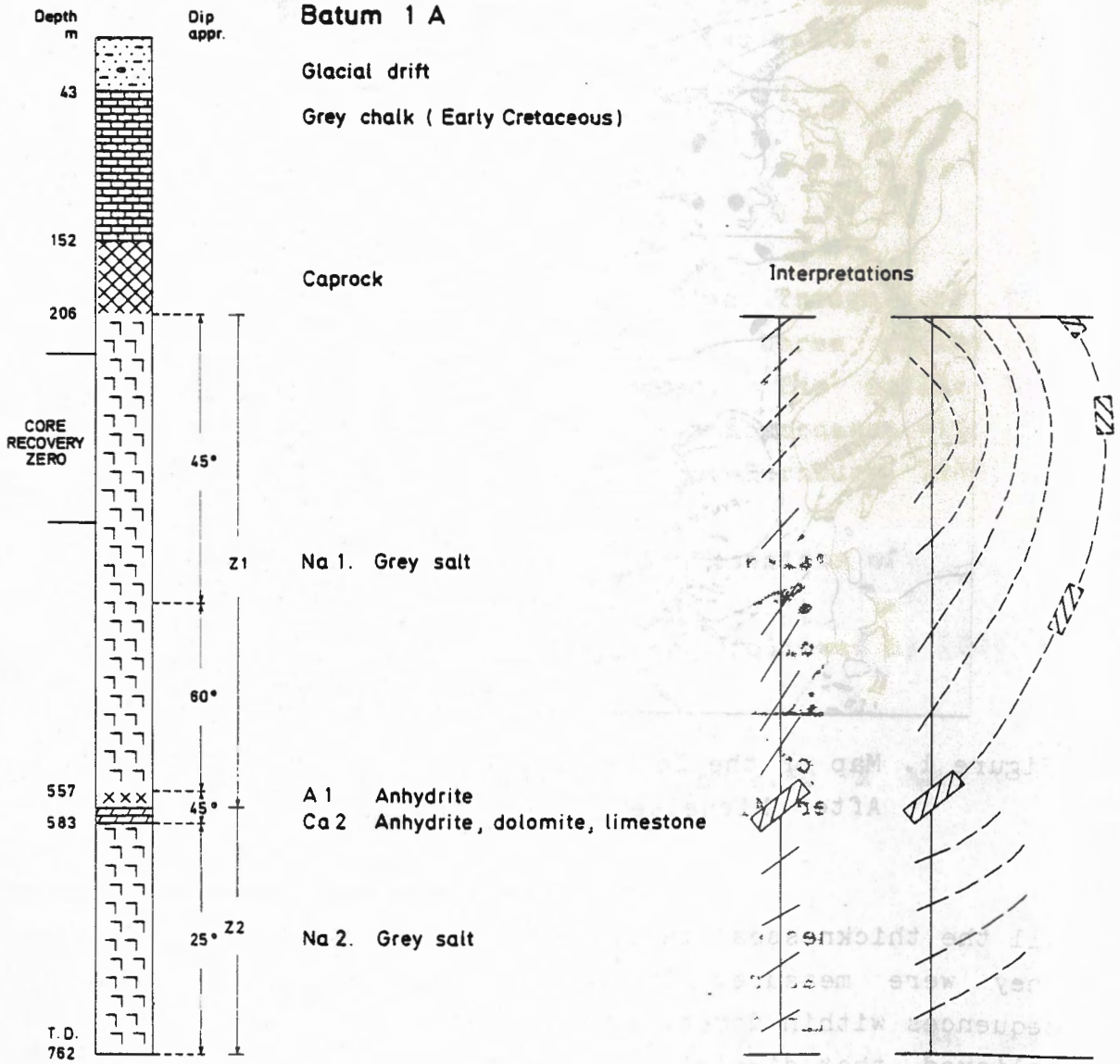


Figure 2. The Batum 1A well. The Z1 and Z2 layers are inverted.

## Materials and Methods.

From a drilled depth of 324 m to TD 752 m 500g of core material was taken at approximately every meter when possible. The salt in the samples was dissolved in hot water and the insoluble residue was treated with heavy fluids in order to extract the quartz crystals. The residue consists of more than 99 % euhedral crystals of anhydrite. The remaining residue consists of:

i. well rounded clastic grains of quartz,

ii. kidney-shaped subhedral to anhedral twins or euhedral to subhedral crystals of kieserite,

iii. euhedral quartz crystals.

### The quartz crystals.

The number of quartz crystals per 500g of core material varies from a few dozens to more than 200. The length of the crystals varies from a few µm up to 1.7 mm. The habit ranges from bipyramids to doubly terminated short and long prismatic forms. The r faces of the bipyramids are as a rule larger than the z faces. Twins of the prismatic type with parallel c-axes and with three or four pyramids are common, and so are small twins of bipyramids with common c-axis.

Righthand or lefthand crystals are rare. The common twins of quartz have not been found.

All the crystals studied have captured one or more small well rounded, clastic grains of quartz. The diameter of the grains rarely exeeds 75 µm. The clastic grains may have acted as crystallization nuclei despite of no visible crystallographic orientation with the host crystal.

All the grains are surrounded by a thin film of brine, which is invisible at room temperature but is disclosed by a small opaque gas bubble. The film becomes semiopaque when frozen due to the formation of ice.

As solid inclusions two types of anhydrite crystals are found. Either as a large number of very small thin tabular crystals with rounded corners forming a poikilitic structure indicating a contemporaneous crystallization of quartz and anhydrite during the early diagenesis (Demangeon, 1966), or a few euhedral tabular crystals, larger than the former, randomly scattered through the quartz crystal. The latter quartz crystals were formed in the salt during the metamorphism that occurred a long time after the end of the diagenesis.

The fluid inclusions.

The fluid inclusions studied are all primary (Roedder, 1976, 1979). Secondary inclusions are extremely rare.

Two types of inclusions are found:

i.
isolated fluid-gas or fluid-gas-solid inclusions, normally

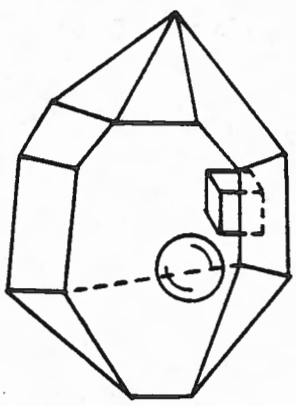


$T_h$ : 106 °C
$T_t$ : 135 °C
$\Delta T$ : 29 °C
P: 32 MPa
Salinity : ~ 40 wt %
Ca : Mg = ~ 1:1
NaCl : 2-3 wt %, 20 °C
4-6 wt %, 135 °C

B1A 1.8.

Figure 3. Fluid-gas-crystal inclusion in perfect crysatllographic orientation with the host crystal.

with a regular shape with sizes up to 35 µm. A single negative crystal in perfect crystallographic orientation with the host crystal was found in a Z1 crystal, figure 3.

ii.
Populations of many, irregular fluid-gas inclusions situated on an internal crystallographic face m, r or z. The inclusions are thin and the irregular shape often exhibits the mosaic structure of the crystal face during the crystallization. Very few of the largest inclusions may contain a cube of NaCl as a daugther mineral, figure 4.

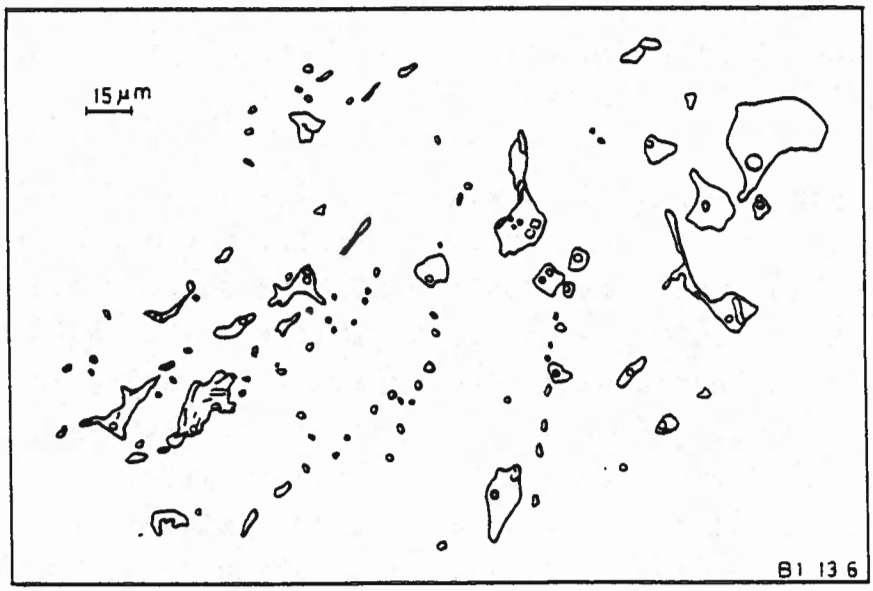


Figure 4. Population of thin irregular inclusions situated on an m interface c.100 µm below the crystal face. Some of the inclusions have a solid phase of NaCl.

As the inclusions as a rule are very thin, the amount of brine may be too small to form a visible cube of halite. The refractive index of halite is very close to the indices of quartz, so a thin "cube" is easily missed. The brines in the inclusions are saturated with respect to NaCl up to the trapping temperature, so if a cube of halite fails to form, the reason also could be a certain oversaturation (metastability).

## Cryometry and Thermometry.

In this fluid inclusion study a 1980 model ChaixMeca cooling-heating device was used.

### Cryometry.

As the solutions are highly concentrated brine consisting mainly of $CaCl_2$ and $MgCl_2$ with subordinate NaCl, the phase diagrams $CaCl_2$-NaCl-$H_2O$ and $CaCl_2$-$MgCl_2$-$H_2O$ (figure 5) by Janat´eva, 1946 combined with the diagrams $MgCl_2$-NaCl-$H_2O$ and ($CaCl_2$+$MgCl_2$)-NaCl-$H_2O$ (figure 6) by Luznaja & Verescetina, 1946 have been used. The last system mentioned is divided into three diagrams depending on the Ca:Mg ratio 3:1, 1:1 and 1:3.

The cryometry procedure was carried out as described by Roedder, 1962: the various melting temperatures were determined "from below" after holding the temperature at -100 °C- -125°C for up to 20 minutes. With slow warming the various hydrates or ice gradually nucleated within the interval -85°C- -65°C. As the salinity is high, ice is rarely formed, and the hydrates completely fill up the inclusion with no gas bubble or visible cube of NaCl. The amount of hydrohalite formed during the freezing run is comparatively small due to the high concentration of $CaCl_2$+$MgCl_2$, so the melting point of the hydrohalite is rarely seen.

The dominating hydrate is $MgCl_2 \cdot 12H_2O$, having refractive indices slightly lower than the indices of quartz. The birefringence is low to moderate.

The hydrate next is either $MgCl_2 \cdot 8H_2O$ or, more often $CaCl_2 \cdot 6H_2O$ depending on the Ca:Mg ratio, figure 5. The optical properties cannot be measured satisfactorily, because the small grains are floating and moving in the fluid. The refractive index is slightly higher than the

index of the surrounding solution with an apparently moderate birefringence.

The diagrams have been used as follows:

The melting temperature of $MgCl_2 \cdot 12H_2O$ is easily

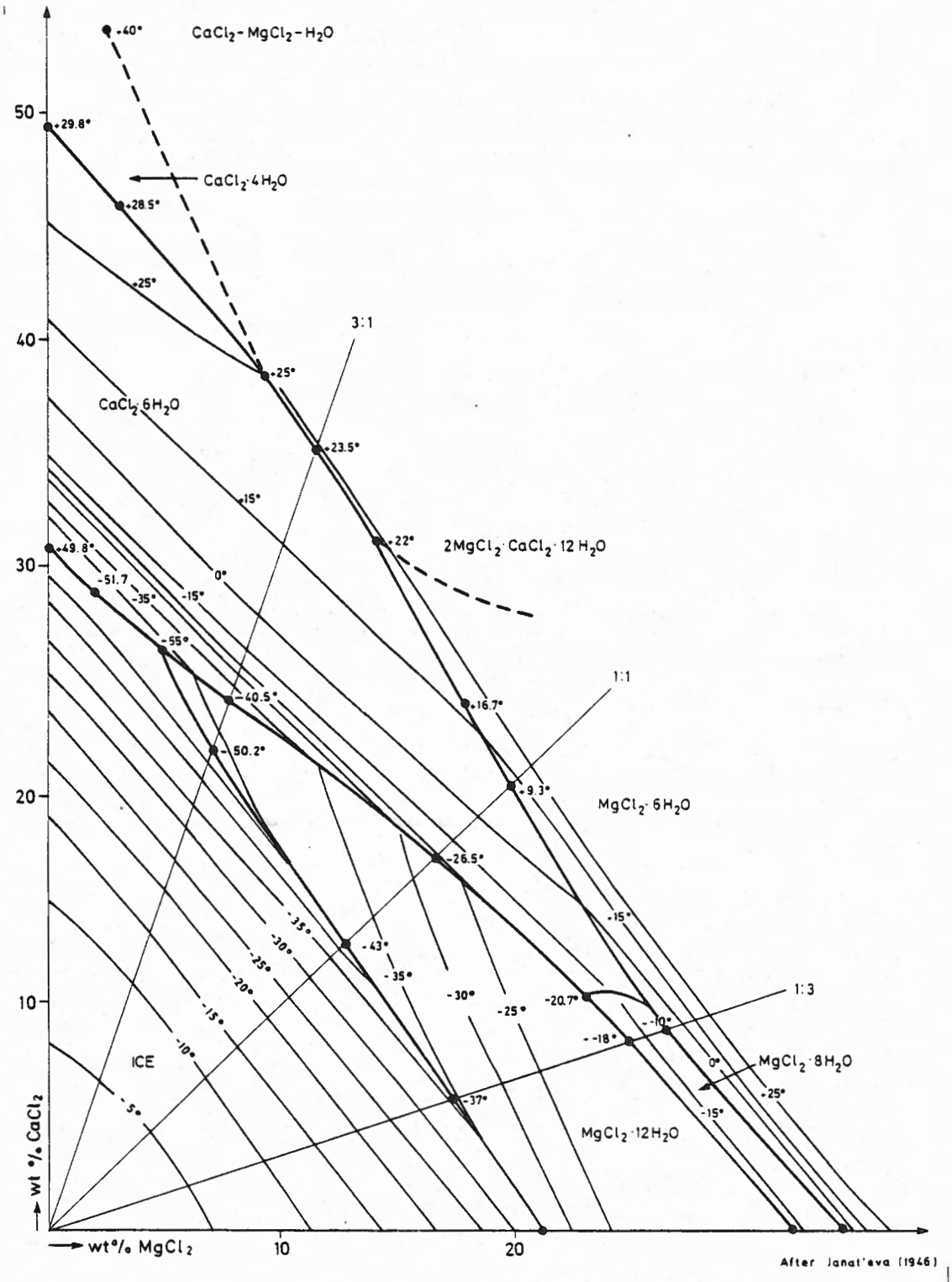


Figure 5. Phase diagram of the system $CaCl_2$-$MgCl_2$-$H_2O$.

recognizable, because comparatively much fluid is released within a small interval of temperature. This melting temperature is indicating the Ca:Mg ratio at the diagrams, figure 6. Between the ratios 3:1, 1:1 and 1:3 the ratio is determined by interpolation at figure 6 and checked at figure 5.

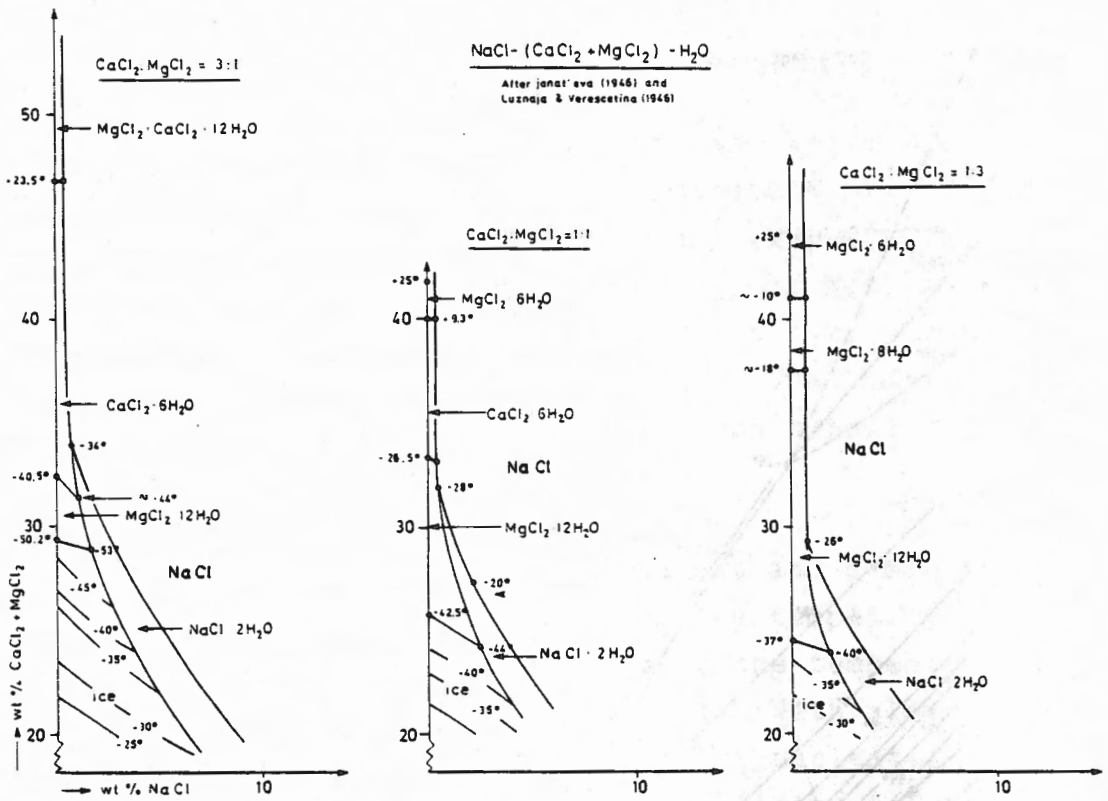


Figure 6. Phase diagrams of the system ($CaCl_2$+$MgCl_2$)-NaCl-H2O, the Ca:Mg ratio 3:1, 1:1, 1:3.

Ratios higher than 3:1 or lower than 1:3 are determined at figure 5.

The melting temperature of the remaining hydrate, either $CaCl_2 \cdot 6H_2O$ or $CaCl_2 \cdot 8H_2O$, is easily determined too, because the hydrate is the only anisotropic solid phase left. This melting temperature gives fairly well the concentration of $CaCl_2$+$MgCl_2$ at the proper ordinate axis at figure 6 and the concentration of NaCl on the abcissa axis, providing that no solid NaCl is present.

Unfortunately the diagrams are not supplied with isotherms in the NaCl field. An estimate of the

concentration of NaCl based on the melting point of the solid NaCl phase can be made from the isotherms in the $CaCl_2$-NaCl-$H_2O$ diagram or from the knowledge of the solubility of NaCl in $CaCl_2$ or $MgCl_2$ solutions at increasing temperature, e.g., Braitsch and Herrmann, 1964, Jenks, 1979, Stewart & Potter, 1979. The determination is defective but it is believed, that the concentration of NaCl does not exeed 8 weight % at the salinity and the melting temperatures measured.

From chemical analyses of brines taken in situ during drilling in Z1 salt, it is known that besides the salts mentioned other ions are present, e.g. Dinesen, 1961:
The Suldrup dome, well No. 8 (at 20°C):

| | NaCl | KCL | $CaCl_2$ | $MgCl_2$ | $Br^-$ | $I^-$ | $NH_4^+$ | $B^{+++}$ | $SO_4^{--}$ |
|---|---|---|---|---|---|---|---|---|---|
| wt % | 3.95 | 3.55 | 15.15 | 8.10 | 0.42 | ---------traces--------- | | | |

The density was 1.29 g/cm$^3$and pH=3.18.

The content of NaCl in situ is increasing with increasing temperature.
During the freezing runs very few inclusions nucleated ice and/or hydrate. The majority of the inclusions did not reacted upon freezing, indicating clean fluids free from nuclei. The explanation may be that the nuclei have settled before the crystallization of the quartz or the selfcleaning effect of quartz during the crystallization has been effective, Grimm, 1962. As the wall rock was NaCl during the crystalization of the quartz, when the fluid inclusions were formed, the fluids must be saturated with respect to NaCl. The concentration of NaCl depends mainly on the trapping temperature, which is unknown for inclusions with no cube of NaCl. The determined salinity of 28 of 231 inclusions (figure 7) may be up to 6-7 weight % too low, whereas the Ca:Mg ratio may be determined satisfactorily. The measured salinity ranges from approximately 35 wt% to more than 45 wt% and the Ca:Mg ratio goes from c.3:1 to c.1:4. The

salinity corresponds with a concentration of seawater from c.50 to more than 100 times, or from NaCl into Mg,K facies, Holser, 1979.

The high Ca:Mg ratios measured may be due to chemical reactions between the original $MgCl_2$ lye and anhydrite, forming $CaCl_2$ enriched solutions, Dinesen, 1961, and kieserite, which is found frequently.

Thermometry.

The homogenization temperature $T_h$, at which the gas bubble disappears, has been measured at 231 fluid-gas inclusions, figure 7. The mean $T_h$=98.1°C +/- 1.1°C, 99%

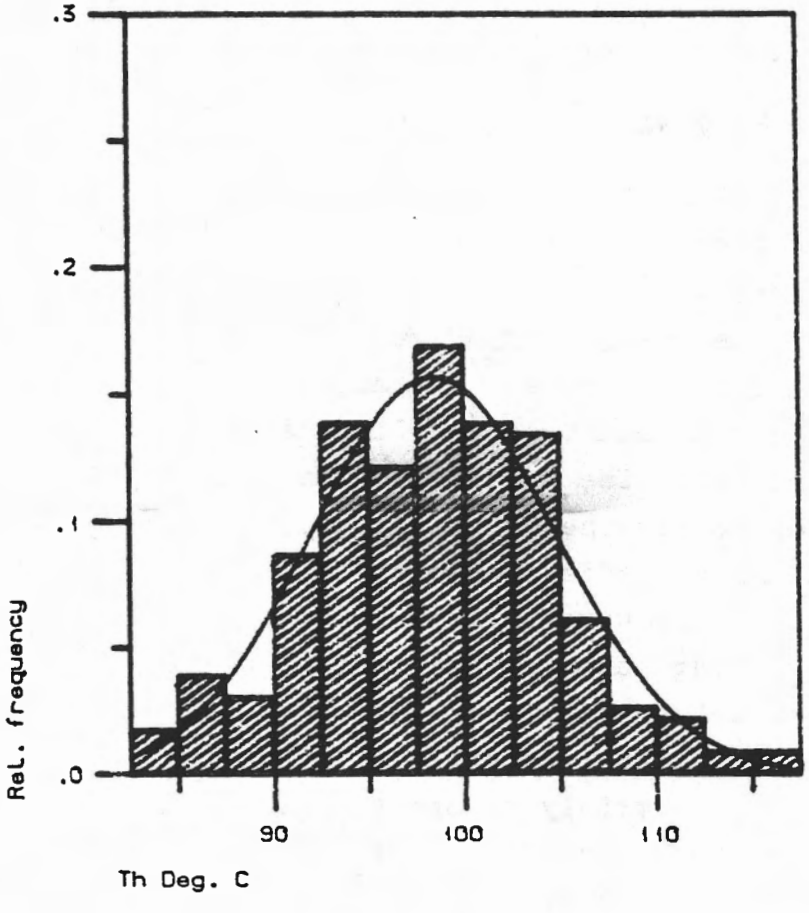


Figure 7.
Homogenization temperatures of 231 fluid-gas inclusions. Mean $T_h$= 98.1°C +/- 1.1°C. 99% confidence limits.

confidence limits. The standard deviation is 6.4°C. As the pressure during the crystallization of the quartz crystals is unknown and as the crystals may have been crystallizing during different conditions a trapping temperature cannot be established.

An obvious trend based on the $T_h$ measurements between Z1 and Z2 cannot have any stratigraphic significance.

The inclusions containing a solid phase of NaCl at room temperature are comparatively large (up to a length of 40 µm) with a comparatively large volume of fluid. The majority of these inclusions is found in connection with smaller inclusions with no visible solid phase of NaCl. As the inclusions are formed at the same time from the same solution, the salinity and the formation temperature must be equivalent. But the temperature $T_h$ is somewhat higher for the fluid-gas inclusions than for the fluid-gas-solid inclusions in the same population.

The quartz crystallized in solutions saturated with respect to NaCl, as the wall rock is halite. Due to this the inclusion fluids also must be saturated with respect to NaCl up to the trapping temperature. Below the trapping temperature a cube of halite is formed in the inclusion. The solution temperature $T_s$ of this cube of halite is the true trapping temperature $T_t$, Touray, 1970. $T_t$ and $\Delta T=T_t-T_h$ of 29 inclusions are noted in table I and II.

Pressure determination.

Several fluid inclusion workers used the so-called "Lemlein-Klevtsov" thermobarometer, that implied an isochoric evolution between $T_h$ and $T_t$ But the T-P path between $T_h$ and $T_t$ is not strictly isochoric, because halite dissolves with a small volume reduction. Roedder and Bodnar, 1980 calculated the corresponding effect with reference to the binary system $NaCl-H_2O$.

However, in strong brines dominated by $CaCl_2$ and $MgCl_2$, the halite solubility is largely depressed due to the "common ion effect". Accordingly, the relative volume of the daughter halite is small and hence, the volume reduction accompanying the dissolution of halite may be neglected.

The pressure P prevailing during the crystallization of the quartz is the pressure determination factor dP/dT multiplied by $\Delta T$, mentioned above: $P = dP/dT \times \Delta T$.

The pressure determination factor is dependent on the salinity and the trapping temperature $T_t$: below a $T_t$ value of 250°C, dP/dT decreases with increasing salinity and increasing $T_t$, Naumov, 1982. Based on the measurements of Naumov extrapolations to the actual values of this work have been performed, figure 8. The measurements are valid for NaCl solutions, but according

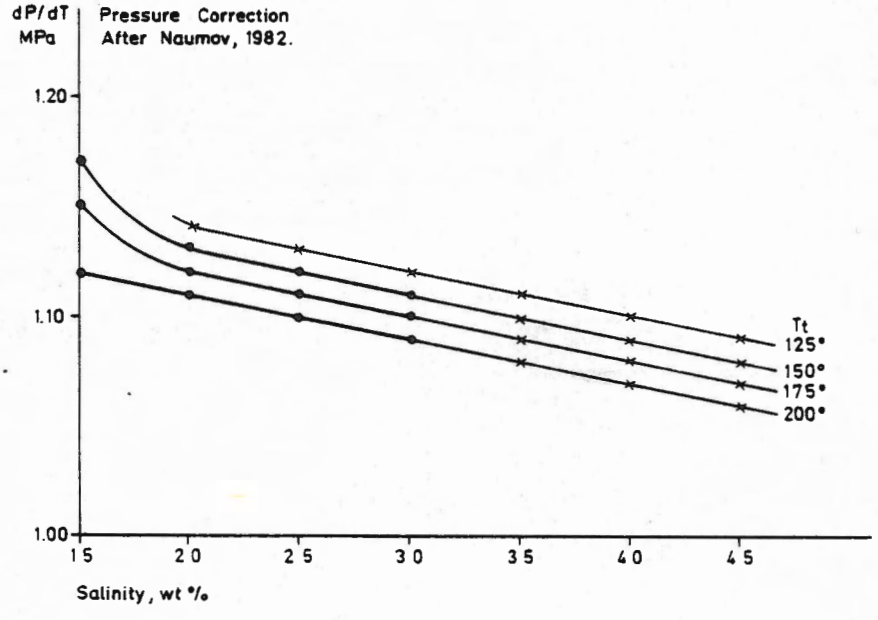


Figure 8. Extrapolations (x) from measured data of Naumov, 1982.

to Haas, 1971 and Potter II, 1977, the pressure correction of $T_h$ in order to estimate $T_t$ can be based on the equivalent NaCl content.

In this work the dP/dT values, noted in tables I and II, have been estimated form figure 8 based on the salinity (eqv. wt% NaCl) and the $T_t$ values, also noted in the tables, (figure 9).

The pressure determination factors used are variable and 10-15% lower than the factors used by Roedder and Belkin, 1977, (12 bars) and by Perthuisot et al., 1978, (12.5 bars per$^{o}$C above $T_h$), cf. Saliot et al., 1978.

The overburden d.

The sedimentary column above the bedded Zechstein salt before the beginning of the diapirism consisted of c.3,300 m of sands and 100-200 m of rocksalt and subordinate clayey material of Triassic age followed by c.900 m of Jurassic and Cretaceous sands and clays. The average density of such unconsolidated and more or less consolidated sediments is c.2.3 g/cm$^3$ according to Dürschner, 1957 and Heroy, 1962.

The quartz crystals studied are found partly in Zechstein 1 near the top of Z1 and partly in Zechstein 2 near the base of Z2. The Zechstein sediments above the quartz in question consisted of 500-700 m of bedded rocksalt and c.100 m of unconsolidated saltclay. The average density of these sediments is c. 2.1 g/cm$^3$.

The total estimated overburden d (km) is calculated from the prevailing pressure during the crystallization of the quartz in connection with the density of the overlying sediments.

The layer A1 of anhydrite in the very top of Zechstein 1 is choosen as the stratigraphic level zero by which the stratigraphic levels S (m) of the different crystals studied are negative in Zechstein 1 and positive in Zechstein 2. The calculated overburden d minus the overburden of Zechstein sediments based on the stratigraphic levels S of the crystal in question gives

the thickness (km) of the post Zechstein (post Z) sedimentary column and thus the time of the formation of the crystal. S, post Z and d are noted in table I and II.

The uncertainty of the average density affects the uncertainty of the determination of the overburden d to some extent.

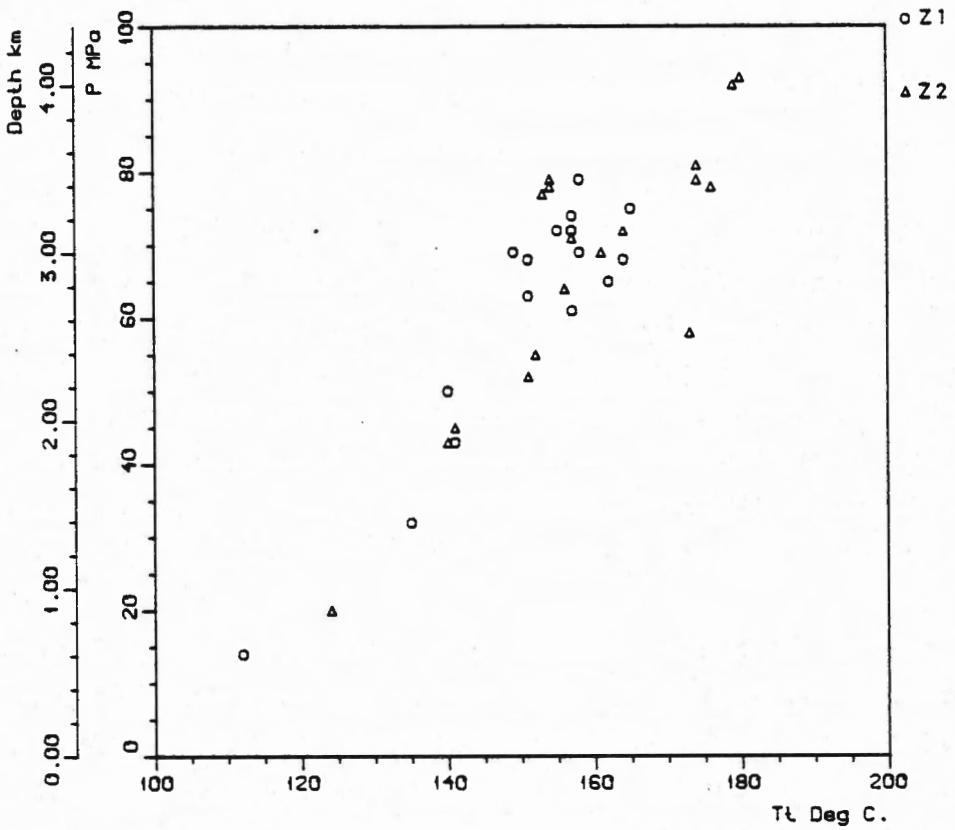


Figure 9. Trapping temperature versus pressure and thickness of overburden of 7 Z1 and 7 Z2 quartz crystals.

The geothermal gradient β .

The uniform vertical temperature gradient β ( $^{o}$C/100 m) was calculated based on the overburden d and the trapping temperature $T_t$, noted in table I and II.

The crystals numbers 8.2 and 10.8 show very high gradients:
19 and 13.8 $^{o}$C per 100 m. respectively. No. 8.2 crystallized at the end of Zechstein times after the

sedimentation of the Z3 salt-clay ( d=0.6 km; post Z=0) and No. 10.8 in the begining of Triassic times after the sedimentation of about 200 m of Triassic sediments (d=0.9 km; post Z=0.2 km). These high gradients must be rather defective; but the seafloor temperature in the Zechstein basin ranges from c.10 °C to c.60°C giving a minimum thermal gradient of c.8 °C/100 m to the site of the two crystals and less than 5 °C/100 m for the entire salt body.

As the thermal conductivity of rocksalt is c.10 times higher than ordinary sediments, these sediments may have acted as an insulating shield, resulting in a thermal build-up in the salt, Talbot et al., 1982. The fairly high temperatures may very likely be explained by repercussions of the Permian volcanism.

The Danish Trough originates from the large transgression of Thuringian (Zechstein) age in consequence of the resumed tectonic movements, e.g. Derumaux, 1980; Ziegler, 1981.

According to Burke and Dewey, 1973 it is beleived, that the Permian faulting in the Norwegian-Danish Basin originated from a plume generated triple junction off N.Jutland, Denmark. The faulting was accompanied by alkaline igneous activity in the Oslo graben. From the junction a "failed arm", the Danish Trough, trends southeast.

The Permian volcanism in the trough is well documented: volcanics directly underlying the Zechstein sediments in well C-1 c.30 km off the westcoast of N.Jutland and in well D-1 c.160 km west of the coast, Rasmussen, 1974. The ages are 237 +/- 16 m.y. and 276 +/- 14 m.y. respectively, Larsen, 1972.

The crystallization temperature of the large majority of the quartz crystals with fluid-gas inclusions solely (figure 7) must be less than the $T_t$= 112°C of crystal No. 8.2, because the large inclusions of these crystals

contain no visible solid phase of NaCl, providing no metastability is present. The calculated overburden d based on these temperatures indicates a crystallization of the crystals not later than Late Zechstein times but also long time after the sedimentation and the diagenesis of the host salt.

Thermal convection.

The probability of thermal convection within a plane horizontal layer of Newtonian fluid with infinite extent, heated uniformly from below depends upon the Rayleigh number R, Talbot, 1978.

The transition from thermal conduction to thermal convection depends on the boundary conditions of the layer in question and is expressed by the critical Rayleigh number $R_c$.

The critical Rayleigh number $R_c$=657 where the top and bottom boundaries are free but inflexible.

Crystalline salt is obviously not an incompressible Newtonian fluid, but is commonly regarded as having an effective viscosity of $10^{13}$ $m^2/s$.

Talbot gives an example in his paper (1978):

For a layer of bedded rocksalt with a thickness of 1,000 m and an overburden of 3,000 m the Rayleigh number was calculated to be R= 768 using a viscosity of $10^{14}$ $m^2$ /s, 10 times higher than the above mentioned.

The conclusion is that R=768 is sufficiently high to suggest that the unstable density gradient induced by the natural heat flow adds significantly to the compositional density inversion previously considered solely responsible for the development of most salt domes.

In the present work the Rayleigh number is expressed by the equation $R = \beta x \underline{d}$ using the physical constants of Talbot's example. $\beta$ is the vertical thermal gradient ($^{o}C$ per 100 m) and $\underline{d}$ is the thickness of the overburden (km) of the crystal in question. Figure 10.

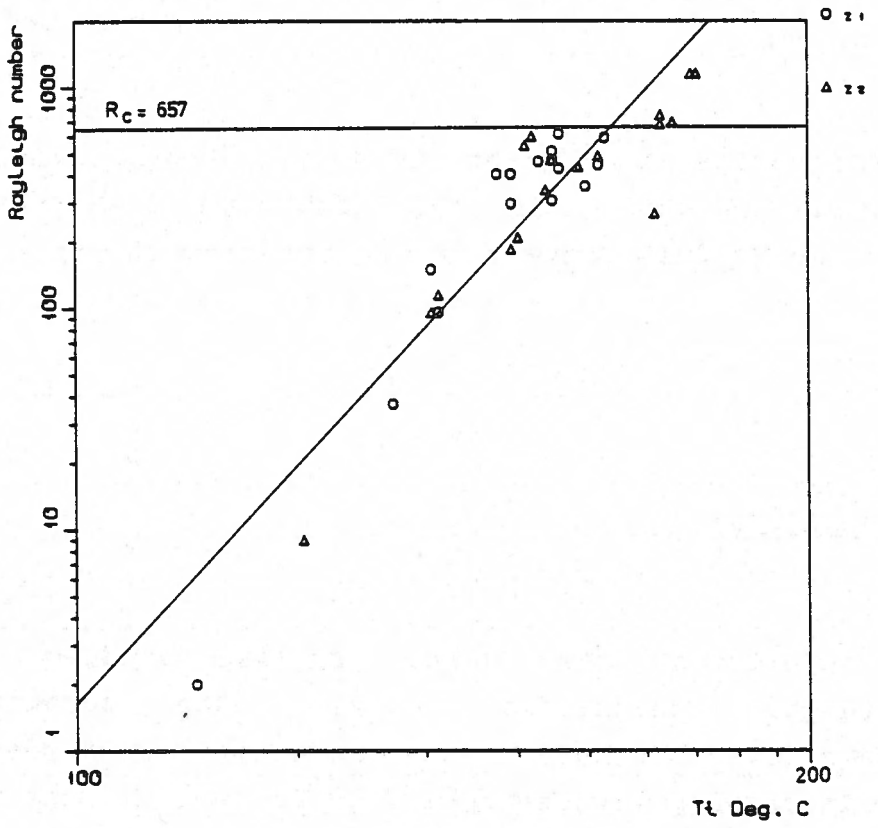


Figure 10. Conditions of thermal conduction below $R_c$ and thermal convection above $R_c$.

The site of crystal No. B.1A.13.6 (table I) was c.100 m above the base of Z2, having an overburden of c.500 m bedded salt and c.3,500 m other sediments. The Rayleigh number calculated is 1152, much higher than $R_c$=657. According to Talbot these thermal conditions are believed to be an important factor in triggering diapirism. In the underlying c.600 m mainly Z1 bedded salt the conditions of thermal convection are even more favourable.

The following conditions in this layer are supposed to give a Rayleigh number higher than 1800:

i. the viscosity is several orders of magnitude less than the viscosity used, because the salt is plastic and "wet", indicated by the formation of the quartz crystals from aqueous solutions.

ii. the pressure and particularly the temperature are higher.

Therefore the conclusion is that strong evidence of thermal convection in the Zechstein 1 salt cannot be overruled. This convection combined with the density inversion may have been active in Late Triassic or Early Jurassic times.

## Conclusions.

The majority of the quartz crystals studied contains fluid-gas inclusions only; the homogenization temperatures of these inclusions exhibit an evident trend of increasing temperature from Z1 to Z2. This trend is believed to be false and may be due to statistical inadequacy.

The measured data: trapping temperature $T_t$, "homogenization" temperature $T_h$, salinity and Ca:Mg ratio do not show any distinct difference between Z1 and Z2 salts. Nor do the derivative calculated data: pressure P, thickness of overburden d, vertical thermal gradient $\beta$ or the Rayleigh number R, which indicate very similar environments during the sedimentation, the diagenesis and the early diapirism of the Z1 salt and the Z2 salt.

The highest Rayleigh numbers calculated indicate conditions of thermal convection in Late Triassic or Early Jurassic times several millions years earlier than the suggested time of the diapiric penetration phase.

ZECHSTEIN 2 TABLE I

| No B.1A | $T_t$ °C | ΔT °C | dP/dT MPa | P MPa | d km | β °C/100m | R | S m | Sal. wt% | Ca:Mg | Post Z km |
|---|---|---|---|---|---|---|---|---|---|---|---|
| 15.7 | 141 | 41 | 1.09 | 45 | 2.0 | 7.1 | 115 | +160 | 40 | 1:1 | 1.5 |
| 13.6 | 174 | 76 | 1.07 | 81 | 3.5 | 5.0 | 750 | +110 | | | 2.9 |
| | 179 | 86 | | 92 | 4.0 | 4.5 | 1152 | | | | 3.4 |
| | 180 | 87 | | 93 | 4.0 | 4.5 | 1152 | | | | 3.4 |
| | 176 | 73 | | 78 | 3.4 | 5.2 | 695 | | | | 2.8 |
| | 164 | 67 | | 72 | 3.1 | 5.3 | 489 | | | | 2.5 |
| | 173 | 54 | | 58 | 2.5 | 6.9 | 269 | | | | 1.9 |
| m | 174 | 74 | | 79 | 3.4 | 5.1 | 682 | | >45 | 1:1 | 2.8 |
| 12.3 | 154 | 73 | 1.08 | 79 | 3.4 | 4.5 | 601 | +90 | | | 2.8 |
| | 153 | 71 | | 77 | 3.3 | 4.6 | 546 | | | | 2.7 |
| m | 154 | 72 | | 78 | 3.4 | 4.5 | 601 | | 45 | 1:1 | 2.8 |
| 11.1 | 151 | 47 | 1.11 | 52 | 2.3 | 6.6 | 185 | +60 | | | 1.7 |
| | 157 | 64 | | 71 | 3.1 | 5.1 | 471 | | | | 2.5 |
| | 161 | 62 | | 69 | 3.0 | 5.4 | 437 | | | | 2.4 |
| m | 156 | 58 | | 64 | 2.8 | 5.6 | 344 | | >35 | 2:1 | 2.2 |
| 10.10 | 152 | 50 | 1.09 | 55 | 2.4 | 6.3 | 209 | +60 | 40 | 1:1 | 1.8 |
| 10.8 | 124 | 18 | 1.09 | 20 | 0.9 | 13.8 | 9 | +50 | 45 | 1:1 | 0.2 |
| 10.5 | 140 | 40 | 1.08 | 43 | 1.9 | 7.4 | 96 | +50 | 45 | 1:3 | 1.2 |

ZECHSTEIN 1 TABLE II

| | | | | | | | | | | | |
|---|---|---|---|---|---|---|---|---|---|---|---|
| 8.3 | 141 | 39 | 1.09 | 43 | 1.9 | 7.4 | 96 | -25 | ? | | 1.2 |
| 8.2 | 112 | 13 | 1.11 | 14 | 0.6 | 19 | 2 | -25 | 42 | 1:1 | 0 |
| 7.14[I] | 140 | 46 | 1.08 | 50 | 2.2 | 6.4 | 150 | -30 | >45 | 2:1 | 1.5 |
| 7.14[II] | 151 | 62 | 1.09 | 68 | 3.0 | 5.0 | 405 | | | | 2.3 |
| | 157 | 66 | | 72 | 3.1 | 5.1 | 471 | | | | 2.4 |
| | 149 | 63 | | 69 | 3.0 | 5.0 | 405 | | | | 2.3 |
| | 158 | 72 | | 79 | 3.4 | 4.6 | 615 | | | | 2.7 |
| | 157 | 68 | | 74 | 3.2 | 4.9 | 514 | | | | 2.5 |
| m | 155 | 66 | | 72 | 3.1 | 5.0 | 462 | -30 | 40 | 1:1 | 2.4 |
| 3.11 | 157 | 56 | 1.08 | 61 | 2.7 | 5.8 | 308 | | | | 1.9 |
| | 164 | 63 | | 68 | 3.0 | 5.5 | 446 | | | | 2.2 |
| m | 162 | 60 | | 65 | 2.8 | 5.8 | 357 | -90 | 45 | 1:2 | 2.0 |
| 1.8 | 135 | 29 | 1.10 | 32 | 1.4 | 9.6 | 37 | -125 | 40 | 3:1 | 0.6 |
| 1.7 | 151 | 58 | 1.08 | 63 | 2.7 | 5.6 | 298 | | | | 1.9 |
| | 165 | 69 | | 75 | 3.3 | 5.0 | 593 | | | | 2.5 |
| m | 158 | 64 | | 69 | 3.0 | 5.3 | 429 | -130 | 45 | 1:1 | 2.2 |

Table I. Measured and calculated data, Zechstein 2.

Table II. Measured and calculated data, Zechstein 1.

Explanations to table I and II:

No.B.1A: Crystal number from well 1A in the Batum dome;

Measured data: $T_t$-trapping temperature, ΔT-trapping temperature minus bubble disappearance temperature; Sal.- Salinity, Ca:Mg ratio.

Calculated data: dP/dT-pressure determination factor; P-pressure; d-thickness of overburden; β-geothermal gradient; R-Rayleigh number; S-stratigraphic level from base Z2; Post Z-post Zechstein overburden.

Acknowledgment.

I want to thank my colleques, F. Lyngsie Jacobsen and J. Gutzon Larsen for the interest and discussions of the methods described here. The work was supported from a grant from the Ministry of Energy (EFP 81).

REFERENCES

Braitsch, O., 1962: Entstehung und Stoffbestand der Salzlagerstätten. Springer-Verlag. 232 p.

Braitsch, O. und Herrmann, A.G., 1964: Konzentrations-, Dichte- und Temperaturverteilung in der Unteroligozänen Salzlagune des Oberrheins. Geol. Rundschau. 54. 344-356.

Burke, K. and Dewey, J.F., 1973: Plume-generated Triple Junctions: Key Indicators in applying Plate Tectonics to old Rocks. Jour. Geol. 81. 406-433.

Demangeon, P., 1966: A propos des quartz authigènes des terrains salifères. Bull. Soc. fr. Mineral. Cristallogr., 89. 484-487.

Derumaux, F., 1980: Le Permien évaporitique de mer du nord relations entre tectonique et sédimentologie. Bull. cent. Rech. Explor. Prod. Elf-Aquitaine. 4. 1. 495-510.

Dinesen, B., 1961: Salt Mineralvand fra Danmarks dybere Undergrund. DGU. IV. Række. 4. Nr. 6. 20 p.

Dürschner, H., 1957: Einige physikalische Überlegungen zum Problem der Halokinese. Appendix to Trusheim, F. (1957). Über Halokinese und ihre Bedeutung für die strukturelle Entwicklung Norddeutschlands. Z. deutsch. geol. Ges. 109. 111-158.

Grimm, W-D., 1962: Ausfällung von Kieselsaure in salinar beeinflüssten Sedimenten. Z. dehtsch. geol. Ges. 114. 590-619.

Haas, J.L., 1971: The Effect of Salinity on the Maximum Thermal Gradient of a Hydrothermal System at Hydrostatic Pressure. Econ. Geol. 66. 940-946.

Heroy, W.B., 1968: Thermicity of Salt as a Geologic Function. Geol. Soc. Am. Special Paper 88. 619-629.

Holser, W.T., 1979: Mineralogy of Evaporites: Marine Minerals. Min. Soc. Am. Short Course Notes, (Burns, R.B. ed.). 380 p.

Janat´eva, O.K., 1946: Polytherms of solubility of salts in the topic system $CaCl_2$ -$MgCl_2$ -$H_2O$ and $CaCl_2$-NaCl-$H_2O$. Jour. apl. Chem. 19. 709-722. (in Russian).

Jenks, G.H., 1979: Effects of temperature, temperature gradients stress and irradiation on migration of brine inclusions in a Salt repository. ORNL-5526. 73 p.

Larsen, O., 1972: Kalium/Argon datering af prøver fra danske dybdeboringer. Dansk geol. Foren. Årsskrift for 1971. 91-94.

Luznaja, N.P. and Verescetina, I.P, 1946: Sodium, calcium and magnesium chlorides in aqueous solutions of -57 to +25 (polythermic solubility). Jour. apl. Chem. 19. 723-733 (in Russian).

Michelsen, O., Saxov, S., Leth, J.A., Andersen, C., Balling, N., Breiner, N., Holm, L., Jensen, K., Kristiansen, J.I., Lair, T., Nygaard, E., Olsen, J.C., Poulsen, K.D., Priisholm, S., Raade, T.B., Sørensen, T.R. and Wurtz, J. 1981: Kortlægning af potentielle geotermiske reservoirer i Danmark. Geol. Surv. Denmark. Ser. B. No. 5. 96 p.

Naumov, V.B., 1982: Possibilities of determination of pressure and density of mineralforming substances based on inclusions in minerals. Laverov ed. Moscow. (in Russian).

Perthuisot, V., Guilhaumou, N. et Touray, J-C., 1978: Les inclusions fluides hypersalines et gazeuses des quartz et dolomites du Trias évaporitique Nord-Tunisien. Essai d´interprétation géodynamique. Bull. Soc. geol. France. 20, no 2. 145-155.

Potter II, R.W., 1977: Pressure corrections for fluid-inclusion homogenization temperatures based on the volumetric properties of the system NaCl-$H_2$ O. Jour. Research U.S. Geol. Survey. 5, No. 5. 603-607.

Rasmussen, L.B., 1974: Some geological results from the first five Danish exploration wells in the North Sea. Geol. Surv. Denmark. III. Ser. No. 41. 42 p.

Richter-Bernburg, G., 1960: Geologischer Bericht über Ergebnis der Bisherigen und Planung der weiteren Exploration auf Kalisalze in Nord-Jütland. Kaliboringerne ved Suldrup 1959-1961. 1. 175 p.

Richter-Bernburg, G., 1981: Geological remarks about the North Jutland salt domes in respect of their suitability for radioactive waste disposal. Unpublished report, ELSAM & ELKRAFT, Denmark.

Roedder, E., 1962: Studies of fluid inclusions I: Low temperature application of a dual-purpose freezing and heating stage. Econ. Geol. 57. 1045-1061.

Roedder, E., 1976: Fluid-inclusion evidence on the genesis of ores in sedimentary and volcanic rocks. Handbook of strata-bound and stratiform Ore Deposits. Wolf ed. 2. 67-110. Elsevier, Oxford.

Roedder, E., 1979: Fluid-inclusions as samples of ore fluids. Geochemistry of hydrothermal ore deposits. John Wiley & Sons. 798 p.

Roedder, E. and Belkin, H.E., 1979: Application of studies of fluid inclusions in Permian Salado Salt, New Mexico, to problems of siting the Waste Isolation Pilot Plant. Scientific Basis for Nuclear Waste Management. 1. 313-321. McCarthy ed. Plenum Press. New York.

Roedder, E. and Bodnar, R.J., 1980: Geologic pressure determinations from fluid inclusion studies. Ann. Rev. Earth. Planet. Sci. 8. 263-301.

Saliot, P., Grappin, C., Guilhaumou, N. et Touray, J-C., 1978: Conditions de formation des inclusions fluides hypersalines de quelques quartz de la "zone des gypses" (Vanoise, Alpes de Savoie). C.R. Acad. Sc. Paris, 286, Serie D. 379-381.

Stewart, D.B. and Potter II, R.W., 1979: Application of physical chemistry of fluids in rock salt at elevated temperature and pressure to repositories for radioactive waste. Scientific Basis for Nuclear Waste Management. 1. 297-311. McCarthy ed. Plenum Press. New York.

Talbot, C.J., 1978: Halokinesis and thermal convection. Nature. 273, No.5665. 739-741.

Talbot, C.J., Tully, C.P. and Woods, P.J.E., 1982: The structural geology of Boulby (potash) mine, Cleveland, United Kingdom. Tectonophysics, 85. 167-204.

Touray, J-C., 1970: Analyse thermo-optique des familles d´enclusions à dépôts salins (principalement halite). Schweiz. Min. Petr. Mitt. 50. H.1. 67-79.

Ziegler, P.A., 1981: Evolution of Sedimentary Basins in North-West Europe. Petroleum Geology of the Continental Shelf of North-West Europe. Institute of Petroleum, London.

# APPENDIX
to
CHAPTER 1 and 2.

In chapter 1 and 2 the diapiric movements have been described as caused by thermal convection as an imaginable mechanism. It is pointed out, that the conditions of thermal convection are present in the bedded rock salt, when the post-Zechstein sediments have a depth of approximately 3500 m.

The thermal convection model is based on the pressure and the temperature in the convecting layer in connection with different physical parameters of the rock salt.

But the measured formation temperatures and the corresponding pressures of the quartz crystals give rise to other models of the diapiric evolution. The first step in this evolution is the pillow stage, which is no longer bedded rock salt in the sense of thermally convecting layers, regardless of the overlying sediments. This stage and the beginning of the diapiric stage may set in when the pressure is at least 400 $kg/cm^2$. (c. 40 MPa), Richter-Bernburg, 1970.

In the diagram below, the quartz crystals studied have been collected in groups named I, II and III. All the crystals, including No. 13.6, were found 300-600 m below the salt miror in the same mass of salt in the well Batum 1A. The overburden consists of c. 200 m of cap rock, Cretacic and Quarternary sediments.

The quartz crystals may have crystallized individually at any time, when the formation pressure and temperature were coinciding with the diagram. Crystals from group I (56 crystals in total) may have formed in Late Zechstein - Early Triassic times as pointed out in chapter 1 and 2. They cannot have been formed recently or in Late Tertiary times, because the crystallization temperatures are too high, even if the pressure is right.

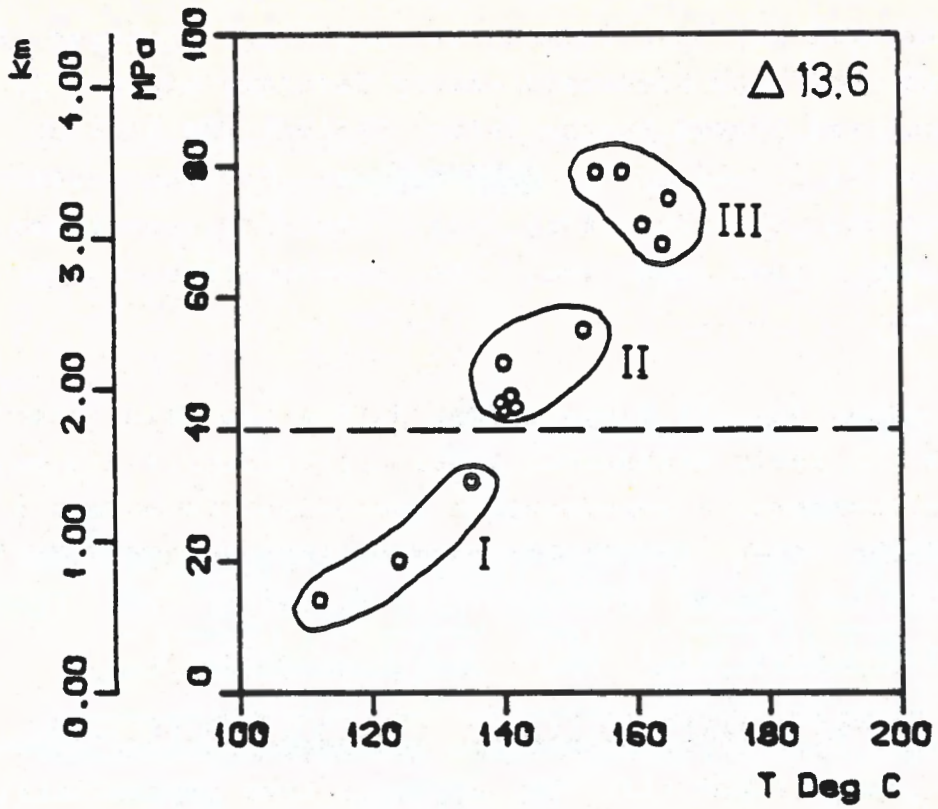


Fig. 1. Crystallization conditions: T versus P.

The large majority of the crystals (53 crystals) of group I crystallized at a mean formation temperature $T_t$ of approximately 110°C and under a pressure of maximum 14 MPa (crystal no. 8.2, chapter 2, table II).

As the stratigraphic site of the crystals in question is close to the transition zone between Zechstein 1 and Zechstein 2 bedded salt, the crystallization of the quartz happened in Late Zechstein times.

The main mechanism of quartz crystallization seems to be the compaction of the salt under a pressure of 10-15 MPa, giving rise to a squeezing out of the highly concentrated bittern brine from the bedded rock salt.

Crystal No. 13.6 attracts particular attention in consequence of the high crystallization temperature ($T_t$ = 180°C) and pressure (P= 93 MPa). In chapter 1 and 2 it is shown, that No. 13.6 crystallized under conditions of thermal convection, if the crystal was formed in bedded rock salt in Late Triassic - Early Jurassic times. But

the crystal may have formed at any time between this period and Late Cretaceous-Early Tertiary times. If the crystal was formed in the latter period, the site of the crystal is lifted up c. 3000 metres. For that reason it cannot be excluded that the diapirism continued in Tertiaty times and that the repercusions still are active.

If crystal No. 13.6 was formed during the main diapiric phase in Early Cretaceous times approximately 1000 metres above basement, a considerable post-diapiric movement in Tertiary times is still needed in order to place the crystal 500 metres below the salt mirror at the finding place.

The same kind of arguments can bed used upon the crystals from group II and III. The crystals have crystallized at any time in the period Early Jurassic-Mid-Tertiary times, when temperature and pressure were in agreement with the measured data.

REFERENCES:

Richter-Bernburg, G., 1970: Contribution to discussion in Geology and Technology of Gulf Coast Salt (Kupfer, D.H. ed.), p. 145.

CHAPTER 3

# THE THERMAL STABILITY OF NATURAL CARNALLITE IN COGNATE GEOLOGICAL ENVIRONMENTS

By Johs. Fabricius

CONTENTS

# THE THERMAL STABILITY OF NATURAL CARNALLITE IN COGNATE GEOLOGICAL ENVIRONMENTS

## ABSTRACT

Natural carnallite ($KMgCl_3 \cdot 6H_2O$) sealed in euhedral quartz from carnallitic rock sequences of the Danish Zechstein evaporites has been studied microthermometrically.

These fluid inclusions represent a closed chemical system containing composite grains and twins of carnallite in connection with $MgCl_2$-KCl solutions saturated with respect to NaCl. The salinity has been found to be from 35 to more than 50 weight%.

The geochemical environment at the time when the quartz crystallized is represented by the sum of the different minerals and fluids trapped during the crystallization. This environment is re-established in a microthermometrical chamber, where the melting/dehydration temperatures have been measured and the corresponding pressures have been calculated. The geochemical environment in situ is represented by the water insoluble residual found in connection with the chemical analyses of the rocks.

The thermal stability of natural carnallite in cognate geological environments increases, and the melting interval narrows, with increasing pressure. The highest melting temperature measured is 182.6°C +/- 0.5°C and the highest pressure calculated is c. 80 MPa +/- 6 MPa.

Approximately one third of the individuals studied melted in the interval 84°C-120°C under vapour pressure, which is supposed to be c. 0.02 - c. 0.05 MPa.

## INTRODUCTION

In continuation of earlier studies of fluid inclusions in euhedral quartz from the Danish Zechstein evaporites, Fabricius (1984) the present work has been carried out on fluid inclusions containing carnallite as the solid phase.
Until the investigation of Kern and Franke (1980, 1981) the knowledge to the thermal stability of carnallite has been restricted to atmospheric pressure or vacuum conditions, e.g., D´Ans and Sypiena (1942); Jockwer (1980). Geller (1930) carried out an investigation of the thermal stability under high pressures: from 165 MPa to 380 MPa corresponding to melting temperatures of 182°C and 201 °C respectively; the work of Kern and Franke was performed by X-ray diffraction on pure carnallite under pressures up to 15 MPa and temperatures up to 200°C.

In order to determine the dehydration conditions of carnallite in situ, it is necessary to perform measurements under in situ conditions in a closed system in which a dynamic equilibrium can be established, Jockwer (1980).

Such closed systems are present as fluid-gas-solid inclusions in euhedral quartz which has crystallized in evaporitic sediments. The inclusions themselves act as natural visual autoclaves. The present work has been carried out with the aid of classic microthermometry on inclusions containing the fossil natural solutions from which carnallite precipitated during the later cooling of the sediments.

## GEOLOGICAL SETTING

In the Danish Subbasin, Zechstein evaporites were precipitated in three main cycles which are believed to correspond to the North German Zechstein 1, 2 and 3 cycles, Richter-Bernburg (1960).

The main potassic rock sequences are found in the upper part of the Zechstein 2 rocksalt, table I. The depths noted are approximate, because they originate from wells in strongly deformed sequences within domes.

TABLE I

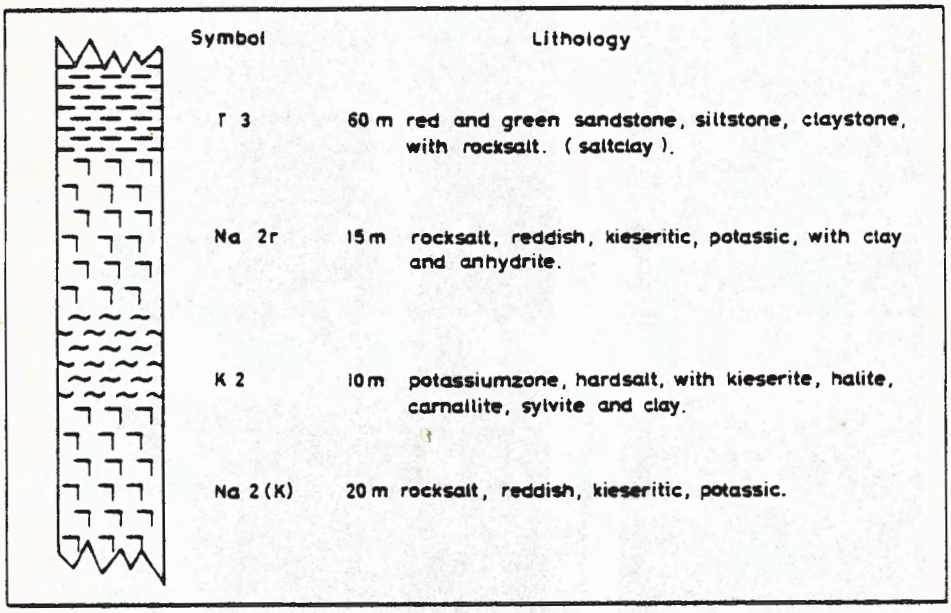

| Symbol | | Lithology |
|---|---|---|
| T 3 | 60 m | red and green sandstone, siltstone, claystone, with rocksalt. ( saltclay ). |
| Na 2r | 15 m | rocksalt, reddish, kieseritic, potassic, with clay and anhydrite. |
| K 2 | 10 m | potassiumzone, hardsalt, with kieserite, halite, carnallite, sylvite and clay. |
| Na 2 (K) | 20 m | rocksalt, reddish, kieseritic, potassic. |

The test material from the carnallite-bearing rocks has been extracted from cores drilled in the Mors dome (well E1, cores Nos. 28, 30 and 31) and the Tostrup dome (well T4, core No. 1; well T10, core No. 14). An example of the rock types is given in figure 1: well E1, core No. 34, the rock types of which correspond with the test material. The salt minerals halite, sylvine and carnallite were dissolved in hot water and the residual, consisting of anhydrite, kieserite, euhedral quartz, hematite, Fe-magnesite, pyrite, clayey material and clastic quartz, was sieved through a 63 micron test sieve. The quartz crystals were separated manually.

The number of quartz crystals is more than 10 times as large as the number of crystals in "the grey salt" Na1 and Na2. They are all long prismatic and many crystals have a tight mosaic structure developed on the m faces. The length of the crystals range from c. 0.2 to c. 1.5 mm with an average length of c. 0.75 mm. Different minerals were captured in the quartz crystal during the crystallization and cavities were formed containing the present fluids.

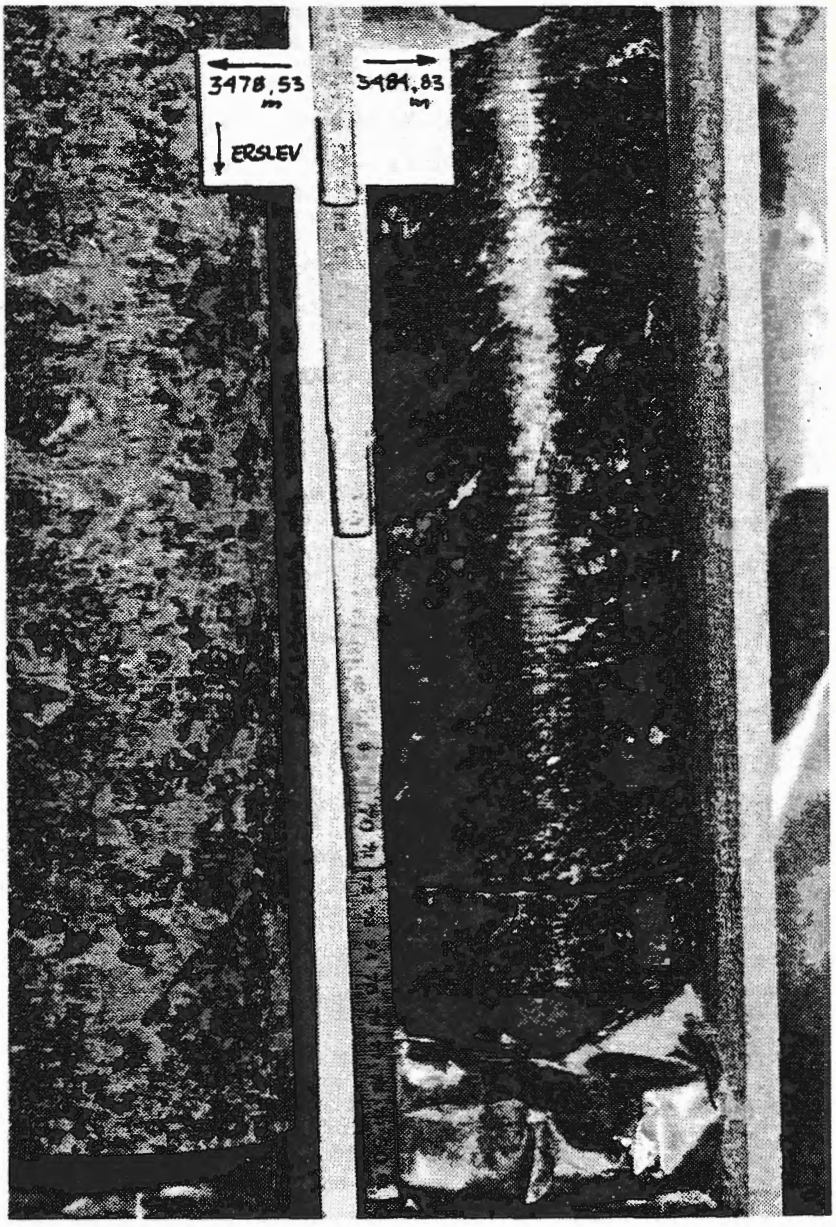


Fig. 1. Salzton T3 and Decksteinsalz Na2r.

The following minerals are trapped: anhydrite, Fe-magnesite, pyrite, euhedral quartz as well as clastic quartz grains, ferric oxidates and clayey material. These minerals and the salts in the fluids reflect the (fossil) geochemical environment when the crystals were formed. During the cooling of the quartz crystals, the dissolved salts in the fluid were crystallized: carnallite, sylvine and halite.

## THE RECENT AND THE FOSSIL GEOCHEMICAL ENVIRONMENTS.

The recent environment, represented by the minerals

present in situ, and the fossil environment, represented by the minerals captured by the quartz during the crystallization, are identical.

The following minerals etc. are common to the two environments:

Primary minerals:

halite
sylvine
carnallite
kieserite
anhydrite, orthorhombic prisms

Accessory minerals:

Fe-magnesite, rhombohedrons
pyrite, octahedrons
quartz, long prismatic crystals
ferric oxidates, red powder
aggregates of quartz crystals intergrown with crystals of Fe-magnesite

Clastics:

clayey material
quartz grains
mica flakes

The crystals are all euhedral crystals with no corrosion on the faces. Kieserite, found in the water insoluble residual as small rounded twins or euhedral crystals, has not been detected as inclusions in the quartz crystals. But as kieserite is a primary mineral, it is believed that kieserite was present in the ancient environment. When pyrite was formed, (in the ancient environment), the pH value was between 5.1 and 7.7 and probably higher than 6.4, as the fluids were in equilibrium with perfect crystals of Fe-magnesite without causing any wear on the crystal faces, Vaughan (1976). As the Fe-magnesite

crystals are unworn in the recent environment too, it is suggested that the pH value was practically the same.

## MICROTHERMOMETRY

### The microthermometrical principle.

When the trapped fluid inclusion, together with the host crystal is cooled down after crystallization, the fluid contracts much more than the quartz and a bubble of vapour is formed. The pressure in the inclusion is equal to the vapour pressure Pvap, depending on the salinity and the temperature. The dissolved salts crystallize, when their precipitation temperatures Tr, are reached during cooling.

The salinity of the fluids is determined by measuring the freezing point depresssion and the melting point of the various hydrates formed during freezing of the studied crystal with the inclusion in connection with the appropriate phase diagrams: the classic cryometry. In order to determine the temperature Tt, at which the inclusion was trapped and hence the quartz crystal was formed, the inclusion is heated until the bubble disappears at the temperature Tb. As long as a bubble is present the pressure is equal to the vapour pressure Pvap. During further heating the pressure in the inclusion increases with a factor dP/dT per $^{o}$C above Tb. Up to the melting temperatures Tm,car, Tm,sy, Tm,ha of the respective solid phases carnallite, sylvine or halite, the phases are in chemical equilibrium with the fluid. The pressure is dP/dT multiplied with (Tm-Tb).

Figure 2 and the five uppermost figures of plate I exhibit the microthermometrical principle. (The hexagonal delineation of the last two pictures of this series on plate I is a reminiscence of the former mosaic structure as well as the form of the inclusion itself in crystallographic agreement with the host crystal).

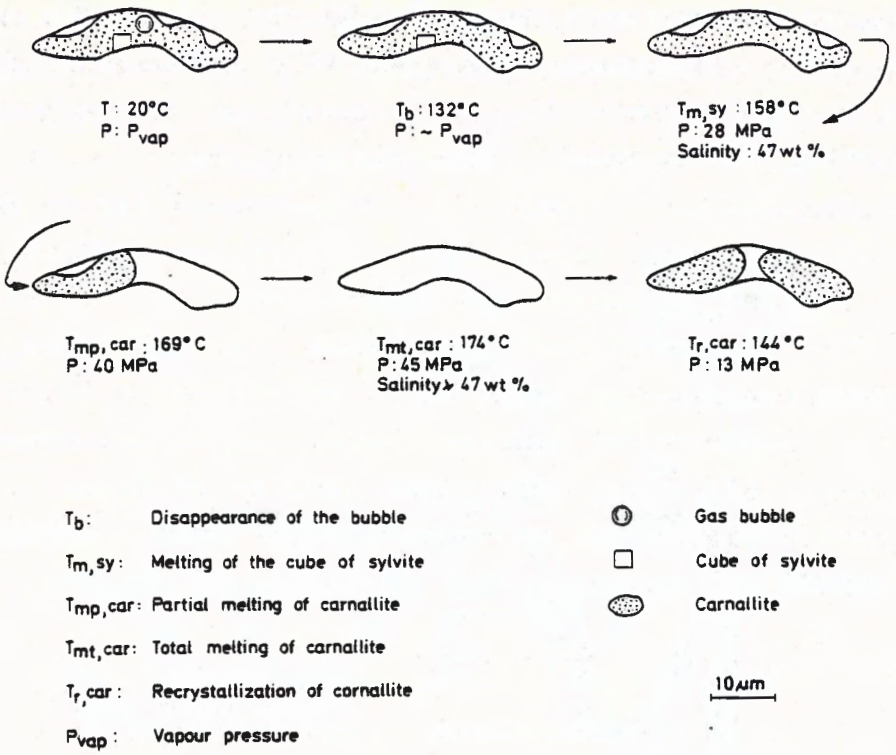


Fig. 2. The microthermometrical principle.

Calibration of the thermometer.

In the fluid inclusion study a ChaixMeca microthermometry apparatus, 1980 model, was used. The heating -freezing stage is commanded by an electronic manual/automatic controller and temperature read-out.
In the thermometer model used, the electronics is constructed in such a way, that after calibration of the apparatus, the read-out is equal to the temperature of the sample.

Determination of the salinity.

In this study the salinity could not be established by the classic cryometry method because only one inclusion reacted upon freezing. The only one reacting formed very little ice while the gas bubble and solution still were present. The melting points of the ice in two runs were -17°C and -19°C respectively.
In a few inclusions, carnallite and sylvine are both present, having the same melting temperature or nearly

so. Using these melting temperatures with a phase diagram of the system $MgCl_2$-KCl-$H_2O$ saturated with respect to NaCl (figure 3), it is possible to establish the salinity fairly well within certain limits.

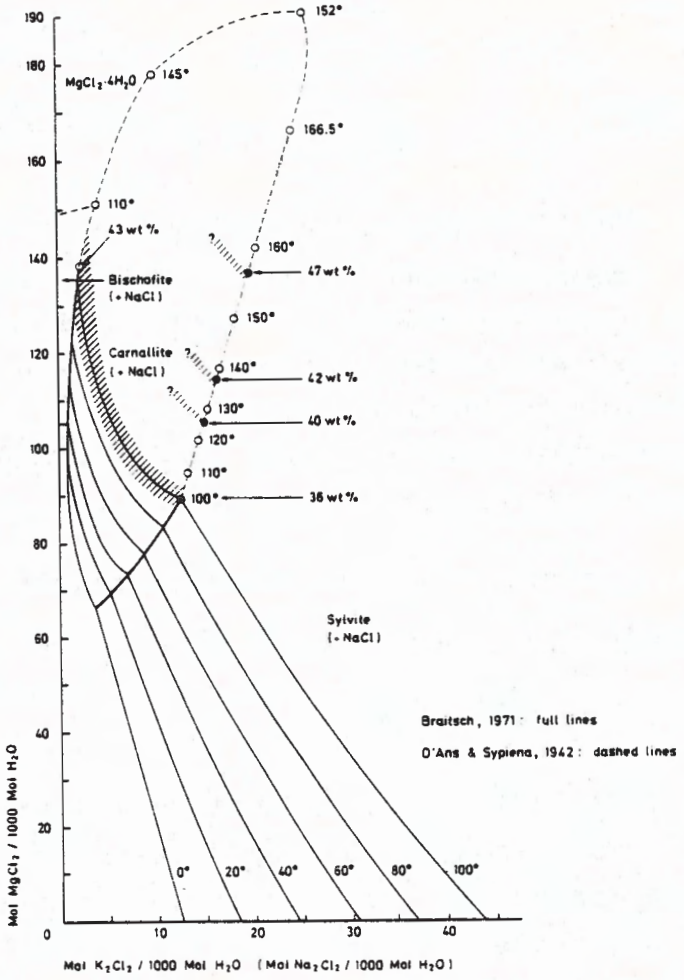


Fig. 3. Phase diagram of the system $MgCl_2$-KCl-$H_2O$, sat. w. NaCl. Modified after D'Ans and Sypiena (1942) and Braitsch (1971).

Determination of the pressure.

The vapour pressure Pvap is dependent on the temperature and the salinity. In this work Pvap has been estimated to be between c. 0.02 and c. 0.05 MPa, Haas (1976); Lorenz et al. (1981).

The pressure determination factor dP/dT is dependent on the concentration of the solutions and the final melting temperature Tm, Naumov (1982).

Below a Tm value of 25o °C the pressure determination factor decreases with increasing salinity and increasing Tm.

Based on the measurements of Naumov, extrapolations to the actual values of this study have been performed, figure 4. The measurements are valid for NaCl solutions, but according to Haas (1971) and Potter II (1977), the pressure correction of Tb in order to estimate Tt≈Tm can be based on the equivalent weight% NaCl content. In this work, the dP/dT values, noted in table II, have been estimated from figure 4 based on the salinity (eqv. wt% NaCl) and the Tm values as also noted in the table.

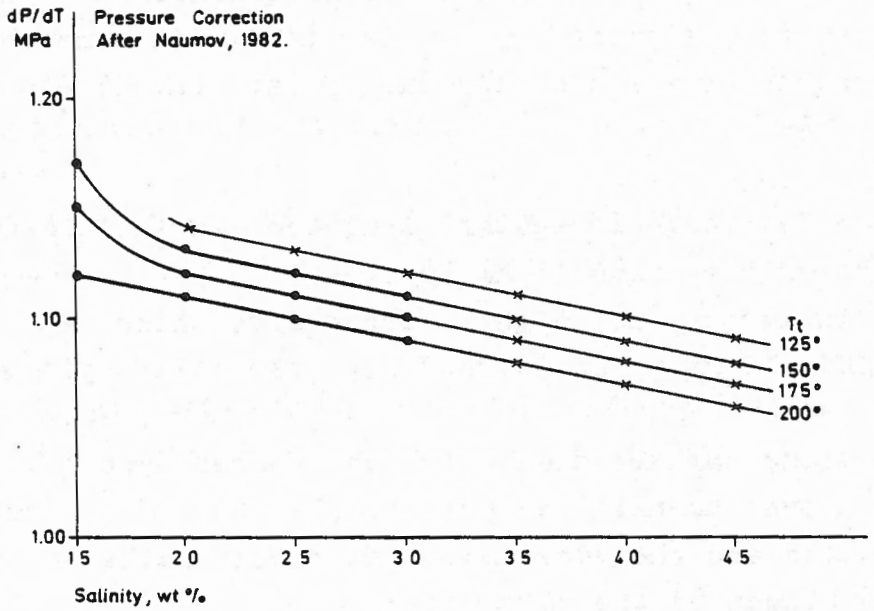


Fig. 4. Extrapolations (x) from measured data of Naumov (1982).

The pressure determination is dependent on the accuracy of the measurement of Tb and the melting temperature Tm,car of the carnallite.

Occasionally, it may be difficult to measure Tb exactly, when the very small bubble disappears in a dark area of the inclusion or it fastens itself to the walls. The determination of Tb is believed to be within +/- 3 °C in these few difficult cases.

An exact determination of Tm,car is easily performed when the carnallite, by manipulating the polariser and the analyser and, if convenient, the gypsum plate, is coloured with a bright luminous colour in contrast to the more or less dark grey or reddish colour of the quartz crystal.

The carnallite-bearing inclusions.

Two types of inclusions are found:

i. small irregular inclusions with a size up to c. 25 μm, as single, isolated inclusions (figure 2) or in small populations situated on a crystallographic interface. In one crystal, a ghost crystal is lined with numerous small inclusions on all the crystal faces (E1.31.2881.I.1-4; table II).

ii. A few large irregular isolated inclusions with a length of more than 75 μm (plate I).
One inclusion is highly irregular, like an amoeba, 200x200x175 μm. (E1.30.2800.I3; table II; plate I).

Inclusions smaller than c. 7 μm are not usable. As a rule, the carnallite practically fills up the entire inclusion and the very small gas bubble fails to nucleate or is hidden by the carnallite.
The carnallite is nearly invisible in plane-polarized light due to the high ratio of carnallite and as a result of the contact between the walls of the inclusion and the surface of the carnallite grains and also the coincidence between the refractive indices of the solution and the carnallite. The disappearance temperature of the gas bubble has been measured on 80 inclusions with no knowledge of the content of carnallite, Fabricius (in press). These temperatures (Th) equal the corresponding temperatures (Tb) of the present work.

Identification of carnallite.

i. the refractive indices of the mineral are less than

the index of quartz and very close to the index of the fluid.

ii. the mineral is often seen in connection with cubes of sylvine.

iii. twins are the rule.

The measurements.

The heating runs were carried out using a heating ratio of 0.5 °C per minute. The carnallite twins or composite grains melted/dehydrated individually, and completely, at various temperatures, like a lump of butter on a warm pan (plate I).

A few individuals in the smaller inclusions melted at one time.
The measured temperatures Tb, Tm,car, Tm,sy and Tr,car are noted in table II together with the calculated pressures.

The histogram figure 5 shows the melting temperature Tm, car of 28 individuals under vapour pressure Pvap.

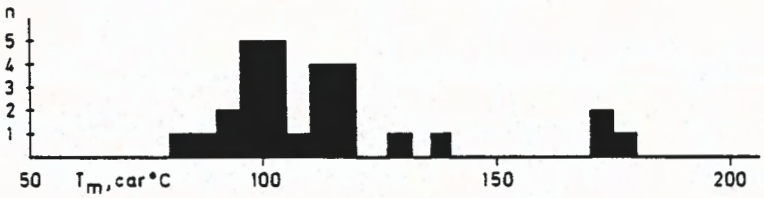


Fig. 5. Tm,car of 28 individuals. Pvap.

In figure 6 Tm,car and the corresponding pressures Pm, car have been plotted.

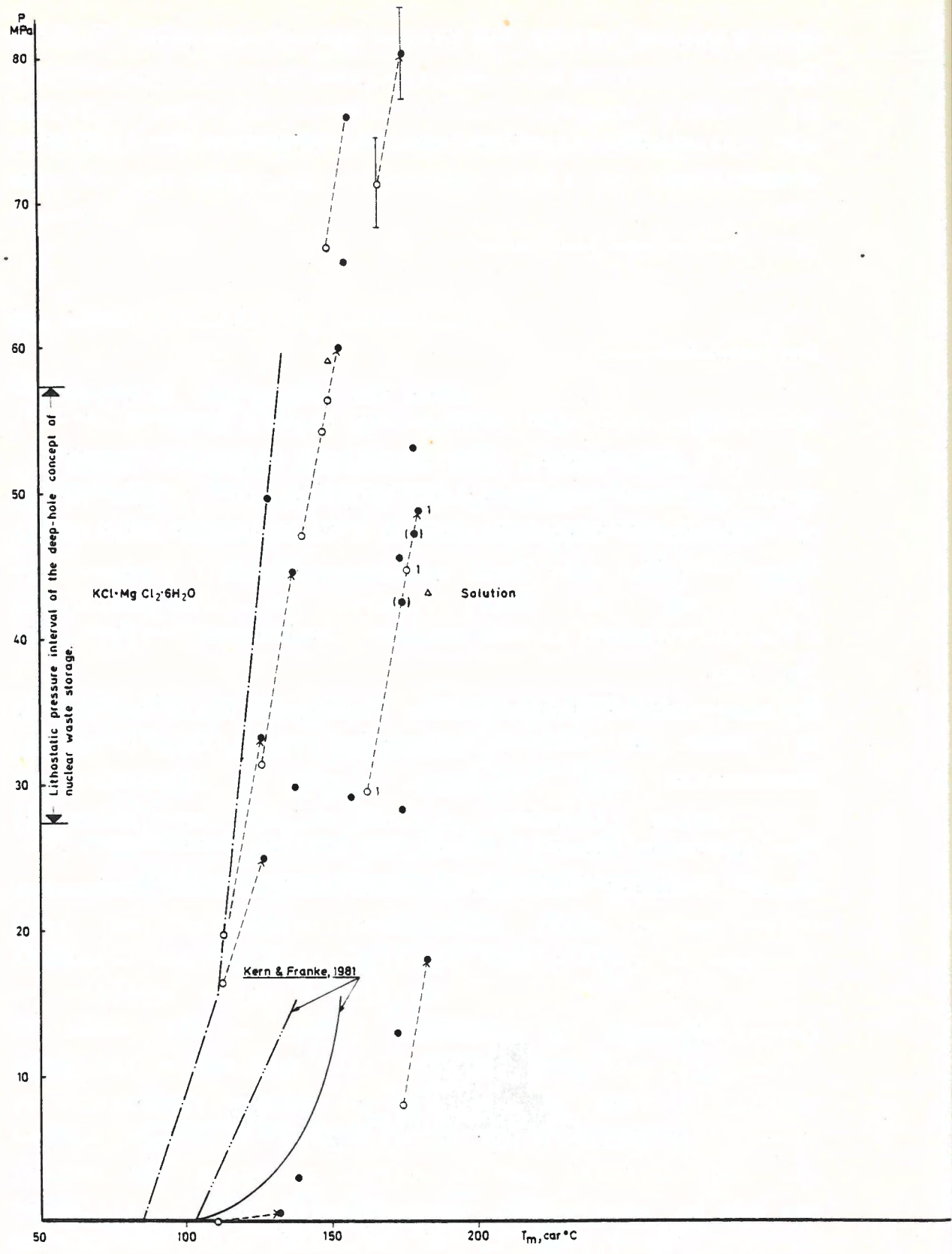


Fig.6. The melting temperature $T_m$,car of the individuals of carnallite versus the corresponding pressure $P_m$,car. The full circles represent the total melting and the open circles the partial melting temperatures of composite grains or twins of carnallite in connection with the calculated pressures. Only a few of the partial melting points of large composite grains have been drawn, e.g. the grain marked "1". The two melting points in brackets derive from a group of three inclusions of which the determination of $T_b$: 100°C +/- 3°C. The one dot broken line is representing the minimum melting temperatures. The open triangles represent minimum formation temperature and pressure of the quartz crystals. The full curve and the double dot broken line are the melting curve and the lower melting limit of the investigation of Kern and Franke,1981.

# TABLE II

| Well No. Core No. Depth m | Crystal No. | Inclusion No. | $T_b$ °C | $T_{m,car.}$ °C | $\Delta T$ °C | dP/dT | $P_{m,car.}$ MPa | $T_{m,sy}$ °C | $T_{r,car.}$ °C | |
|---|---|---|---|---|---|---|---|---|---|---|
| E1 | I | 1 | 134.5 | 162.3 | 27.8 | 1.07 | 29.7 | | | individual melting, |
| 28 | | | | 176.4 | 41.9 | | 44.8 | | | grain by grain |
| 2713 | | | | 180.1 | 45.6 | | 48.8 | | | |
| | | 2 | (134.5) | 159.1 | 24.6 | | 26.3 | | ~ 125 | Neighbour to no 1, |
| | | | | 167.9 | 33.4 | | 35.7 | | | bubble disappears |
| | | | | 174.3 | 39.8 | | 42.6 | | | in dark area. |
| | | 3 | (134.5) | 164.0 | 29.5 | | 31.6 | | | Neighbour to No. 1, |
| | | | | 178.7 | 44.2 | | 47.3 | | | bubble disappears in dark area. |
| E1 | I | 1 | 131.5 | 174.2 | 42.7 | 1.07 | 45.7 | | 135.4 | |
| 30 | | 2 | 129.8 | 179.4 | 49.6 | | 53.1 | 171.6 | 103.9 | |
| 2800 | | 3 | (>200) | 172.3 | | | Pvap | (~215) | 147.7 | is leaking. Dehyd. 84°, 110°, 115°. $T_m$,ice:-19°C. |
| | III | 1 | 169.5 | 99.1 | | | Pvap | ~ 50 | | |
| | | 2 | ? | 104.9 | | | " | | ~ 90 | |
| | | 3 | ? | 127.3 | | | " | | ~ 85 | |
| | IV | 1 | 130.3 | 157.3 | 27.0 | 1.08 | 29.2 | | | |
| | | 2 | 159.9 | 171.8 | 11.9 | 1.07 | 12.9 | | | |
| | | 3 | 147.8 | ~115 | | | Pvap | | | |
| | | | | 174.2 | 26.4 | 1.07 | 28.2 | | 152.8 | |
| | VI | 1 | 97.1 | 126.7 | 29.6 | 1.08 | 32.0 | | | |
| | | | | 140.6 | 43.5 | | 47.0 | | | |
| | | | | 147.4 | 50.3 | | 54.3 | | | |
| | | | | 148.5 | 51.4 | | 55.5 | | | |
| | | | | 153.1 | 56.0 | | 60.5 | | 130.3 | |
| | VII | 1 | ~195 | 108.7 | | | Pvap | | | has leaked |
| | | | | 113.6 | | | " | | | |
| | | | | 117.6 | | | " | | 97.8 | |
| | | 2 | 143.0 | 87.4 | | | Pvap | ~100 | | salinity ~36 wt% |
| | | | | 101.2 | | | " | | | |
| | | 3 | ~145 | 96.7 | | | Pvap | | | |
| | | | | 101.0 | | | " | | | |
| | VIII | 1 | 130.6 | 104.7 | | | Pvap | | | |
| | | | | 131.1 | 1.5 | 1.08 | 0.5 | | ~ 90 | |
| | IX | 2 | 165.8 | 173.4 | 7.6 | 1.07 | 8.1 | | | |
| | | | | 182.6 | 16.8 | | 18.0 | | | |
| | | 3 | ~133 | 114.3 | | | Pvap | | ~ 85 | |
| | | 4 | >180 | 115.9 | | | Pvap | | ~ 85 | |
| | X | 1 | ~100 | 166.8 | (66.8) | 1.07 | (71.5) | | | |
| | | | | 175.2 | (75.2) | | (80.5) | | | |
| | | 2 | 93.5 | 155.4 | 61.9 | | 66.0 | | | |
| | | 3 | 97.3 | 112.6 | 15.3 | | 16.4 | | | |
| | | | | 120.7 | 23.4 | | 25.0 | | | |
| | | 4 | 86.7 | 149.2 | 62.3 | | 66.9 | | | |
| | | | | 157.7 | 71.0 | | 76.0 | | | |
| | | 5 | ?dry | 164.3 | | | ?Pvap | | | 1st heating run of |
| | | | | 178.0 | | | " | | | the crystal. |
| | | | | 178.6 | | | " | | | |
| | | | >200 | 172.5 | | | Pvap | | | 2nd run, leaks out |
| | | | | 178.4 | | | " | | | in water film around clastic quartz grain |
| E1 | V | 1 | 158.2 | 98.2 | | | Pvap | 93.4 | | salinity ~36 wt% |
| 30 | | 2 | 148.4 | 97.2 | | | " | | ~ 95 | |
| 2802 | | 3 | 172.0 | 91.0 | | | " | | ~ 90 | |
| | | 4 | 164.7 | 96.9 | | | " | | ~ 95 | |
| | | 5 | 170.9 | 90.8 | | | " | | ~ 90 | |
| | VI | 1 | 153.8 | 138.5 | | | " | | | |
| | | 2 | 136.6 | 138.5 | 1.9 | 1.08 | 2.2 | | | |
| | | 3 | 178.2 | 101.9 | | | Pvap | 105.8 | | salinity ~36 wt% |
| E1 | I | 1 | 79.5 | 129.2 | 49.7 | 1.08 | 53.7 | | | |
| 31 | | 2 | 159.2 | 111.2 | | | Pvap | | | |
| 2881 | | 3 | 95.9 | 114.4 | 18.5 | | 20.0 | | | |
| | | | | 126.8 | 30.9 | | 33.4 | | | |
| | | 4 | 96.0 | 125.1 | 29.1 | | 31.4 | | | |
| | | | | 137.4 | 41.4 | | 44.7 | | ~ 105 | |
| T10 | I | 1 | 110.3 | 137.7 | 27.4 | 1.08 | 29.6 | | | |
| 14 | | | | | | | | | | |
| 1402 | | | | | | | | | | |

$T_b$: disappearance temperature of the gas bubble. $T_m$,car: melting temperature of carnallite. $\Delta T$: $T_m$,car - $T_b$. dP/dT: pressure determination factor. $P_m$,car: pressure at $T_m$,car. $P_{vap}$: vapour pressure. $T_m$,sy: melting temperature of sylvine. $T_r$,car: recrystallization temperature of carnallite.

# DISCUSSION.

The quartz crystals crystallized in a silica-saturated $MgCl_2$-KCl solution saturated with respect to NaCl.

In two crystals, fluid inclusions containing a cube of NaCl as the only solid phase were found. Such inclusions give rise to the determination of the quartz crystallization temperature and the prevailing pressure during the crystallization, Fabricius (1984).

During crystallization the solution had a minium temperature of 180 C and the minimum prevailing pressure was of 60 MPa. The results are shown as open triangles on the diagram, figure 6.

The pressure corresponds to an overburden of about 2500-3000 m of sediment which indicates that the formation of the quartz crystals took place late in Triassic or Early Jurassic times, maybe during the initial phase of the pillow stage or the diapiric movement. The fairly high temperatures may perhaps be explained by repercussions of the Permian volcanism, Fabricius (1984).

The carnallite-bearing inclusions were trapped by the quartz crystals during the crystallization, i.e., the temperature of the solutions was a minimum of $180^{\circ}C$.

The carnallite was dissolved in the solution and was not a solid phase during trapping. As the carnallite nearly fills up the inclusions, the concentration of $MgCl_2$ and KCl in the fluid must have been high. All other solid inclusions such as pyrite, quartz crystals etc. are not in contact with any solution, except clastic quartz grains, which always are surrounded by a mild brine.

Five of the tested inclusions also have, besides carnallite, a cube of sylvine at $20^{\circ}C$: the solution is saturated with respect to KCl up to the melting temperature of the sylvine in these five inclusions.

Carnallite melts incongruently at 167.5 °C under atmospheric pressure, forming a solution and KCl, D´Ans and Sypiena (1942). This formation of KCl has not been observed, even at melting temperatures higher than 167.5 °C. This may be due to a heating rate that was too high (though the heating rate was held as low as 0.5 °C per minute) or that all the KCl has been used in forming the carnallite which is surrounded by a KCl deficient $MgCl_2$-solution.

Approximately 45% of the carnallite individuals melted under vapour pressure. This observation is hard to explain, because the inclusions represent a closed system. More than 80% of these individuals melted at temperatures in the interval 84 °C-120 °C (figure 5). The mean temperature of this group is 101 °C.
The group represents c. 35% of all individuals studied.

Inclusion E1.30.2800.I.3 (table II, plate I) was studied after three or four heating runs at inclusion No. 1 and 2. As the inclusion is close to the surface of the crystal, the inclusion may have leaked through microjoints caused by the high pressures during the heating runs. The carnallite composite grain melted individually under vapour pressure at 84 °C, 110 °C, 115 °C etc. and the last individual finally melted at 172.3 °C with some gas bubbles still present.
During the melting of the last individual some crystals of KCl were discovered. These crystals melted crystal by crystal from c. 190 °C and the last crystal melted at c. 215 °C. The last gas bubble disappeared at c. 205 °C. Since a very small amount of gas (e.g. $CO_2$,$N_2$ etc) can be dissolved in solutions with a salinity higher than 40 weight%, an explanation of the presence of high-pressure gas in the gas bubbles is invalidated. Perhaps this inclusion exhibits the only example of incongruent melting in connection with a high concentration of KCl. The vapour pressure in this case is believed to be much higher than 0.05 MPa due to the salinity and the temperature.

The phase diagram, figure 2, can only be used to

determine the salinity under atmospheric pressure conditions. As the melting temperature of carnallite is increasing with increasing pressure and since pressures much higher than atmospheric pressure have been calculated during this investigation, the diagram shows tendencies only. The measurements are indicated at figure 2 with a black dot and the isotherms with hatched areas.

The salinity after melting of carnallite and sylvine is determined from c. 35 to more than 50 weight% $MgCl_2$-KCl-NaCl solution, saturated with respect to NaCl.

Quartz crystals from the Hartsalz (K2) are all strongly etched on the m faces, which is believed to be due to the highly kieseritic solutions depositing the kieserite as Hartsalz. If this theory is true, then the quartz crystals are older than the formation of the kieserite.

As kieserite is not believed to influence the dehydration behaviour of carnallite, Kern and Franke (1981), the dehydration behaviour found in this study is interpreted as being valid for carnallite in situ in the recent geochemical environment.

The carnallite grains have all been "wet" carnallite, i.e., surrounded by solution. Inclusion E1.30.2800.X.5 placed in a small cavity of a clastic quartz grain is supposed to be "dry" carnallite during the first heating run. During the following cooling the carnallite recrystallized into the brine film surrounding the quartz grain. During the next heating run the carnallite was "wet". The melting temperatures measured during the two runs show no significant differences (table II).

Kern and Franke (1981) have carried out an investigation of the thermal stability of pure carnallite and of carnallite powder coexisting with halite and kieserite by means of a PT-X-ray technique. The maximum temperature was 200 °C and the maximum pressure was 15 MPa. The conclusion is that thermally-induced released

water from the carnallite structure is highly dependent on pressure, and on the partial water pressure in particular. It is inferred that release of small amounts of structurally-bound water increases the partial water pressure within intra- and inter-crystalline pore spaces, thereby shifting the dehydration temperature to significantly higher values. In figure 6 the lower and the upper limit (the melting curve) of the dehydration field have been constructed . Similarly the lower limit of the present work is showed in figure 6. Due to the small number of observations the upper limit, the melting curve, could not be constructed, and no reliable statistics carried out. But despite the few observations the trend is marked: the thermal stability of carnallite increases with increasing pressure and the melting interval narrows.

Many of the quartz crystals studied in the present work were found lining small vugs (Ø 2-3 mm) in the clayey material and due to this it is believed that sealed pores and intergranular spaces which contain carnallite and solution may be present in situ in rocks free from cracks and microjoints.

The formation temperature in situ of the deep-hole concept of nuclear waste storage (1200-2500 m) is c. 45 $^{o}$C and c. 65$^{o}$C respectively (well E1 in the Mors dome). The difference between the minimum melting temperature and the formation temperature in situ is 70-75$^{o}$C.

Approximately one third of the carnallite individuals studied melted under vapour pressure at temperatures within the interval 84-120$^{o}$C (average c.100 $^{o}$C) in a closed system. The minimum temperature differences are c. 55$^{o}$C (1200 m) and c. 35$^{o}$C (2500 m).

## CONCLUSIONS

The fossil geochemical environment does not differ significantly from the recent environment.

The thermal stability of natural carnallite in cognate geochemical environments increases with increasing pressure and the melting intervals become narrower. When the carnallite melting under vapour pressure is neglected, the beginning of the dehydration takes place at much lower temperatures than previously suggested.

It is believed that these observations on the behaviour of carnallite in a closed system with increasing pressure and temperature indicate an insufficient understanding of the nature of the in situ behaviour.

The thermal conditions must be taken into account when calculating safety distances in connection with heat-generating waste in mines or deep holes.

Due to the few observations, a melting curve cannot be established and therefore the results cannot be treated in a statistically satisfactory way.

## REFERENCES


D´Ans, J. und Sypiena, B., 1942: Löslichkeiten im System $KCl-MgCl_2-H_2O$ und $NaCl-MgCl_2-H_2O$ bei Temperaturen bis etwa $200^0$. Kali u. Erdöl. 89-95

Braitsch, O., 1971: Salt Deposits, their Origin and Composition. Springer-Verlag 297 pp.

Fabricius, J., 1984: Formation temperature and chemistry of brine inclusions in euhedral quartz crystals from Permian salt in the Danish Trough. Bull. Mineral. 107. 203-216.

Fabricius, J., in press: Studies of fluid inclusions in halite and euhedral quartz crystals from salt domes in the Norwegian-Danish Basin. Sixth international Symposium on Salt.

Geller, A., 1930: Das Schmelzen von Salzen bei hohen Drucken in seiner Bedeutung für den Vorgang der Salzmetamorphose. Fortschr. d. Mineralogie. 14. 143-166.

Haas, J.L. Jr., 1971: The Effect of Salinity on the Maximum Thermal Gradient of a Hydrothermal System at Hydrostatic Pressure. Econ. Geol. 66, 940-946.

Haas, J.L.Jr. 1976:Physical Properties of the Coexisting Phases and Thermochemical Properties of the H.O Component in Boiling NaCl Solutions. Geol. Surv. Bul. 1421-A. 73 pp.

Jockwer, N., 1980: Die thermische Kristallwasserfreisetzung des Carnallits in Abhängigkeit von der absoluten Luftfeuchtigkeit. Kali u. Steinsalz. 8. 2. 55-58.

Kern, H. und Franke, J-H., 1980: Thermische Stabilität von Carnallit unter Lagerstättenbedingungen. Glückauf-Forschungshefte. 6. 252-255.

Kern, H. und Franke, J-H., 1980: The effect of temperature on the chemical and mechanical behaviour of carnallite-halite rocks. Trans. Tech. Publ. Penn. State Univ. 1-11.

Lorenz, J., et al., 1981: Geology, Mineralogy, and Some Geophysical and Geochemical Properties of Salt Deposits. in Physical Properties Data for Rock Salt. Gevantman, L.H. ed. NBS Monograph 167. 286 pp.

Naumov, V.B., 1982: Possibilities of determination of pressure and density of mineral forming substances based on inclusions in minerals. Laverov ed. Moscow. 85-93. (in Russian).

Potter II, R.W., 1977: Pressure corrections for fluid-inclusion homogenization temperatures based on the volumetric properties of the system NaCl-$H_2O$. Jour. Research U.S. Geol. Surv. 5. No. 5. 603-7.

Richter-Bernburg, G., 1960: Geologischer Bericht über Ergebnis der Bisherigen und Planung der weiteren Exploration auf Kalisalze in Nord-Jütland. Kaliboringerne ved Suldrup 1959-1961. 1. 175 pp.

Vaughan, D.J., 1976: Sedimentary geochemistry and mineralogy of the sulphides of Pb, Zn, Cu and Fe and their occurence in sedimentary ore deposits. In Handbook of strata-bound and stratiform ore deposits, Wolf, K.H. ed. 2. 317-363.

PLATE I

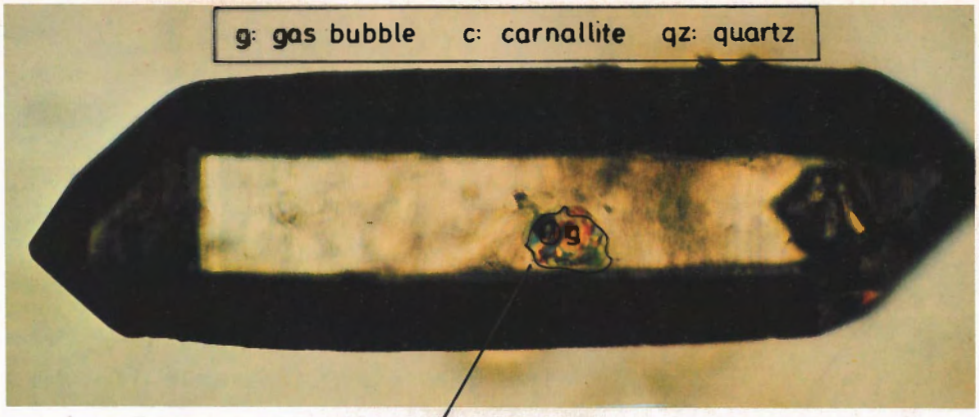


Quartz crystal E1.30.2800.IV, ø 80 µm. T: 20°C

945 x 270 µm, with inclusion No. 3,

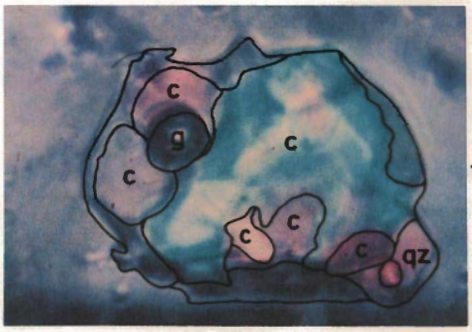


T: ~115°C. $P_{vap}$

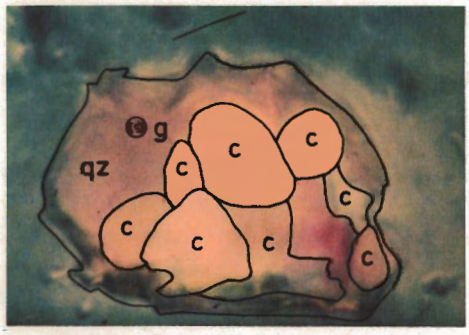


T: ~140°C. $T_b$: 147.8°C $P_{vap}$

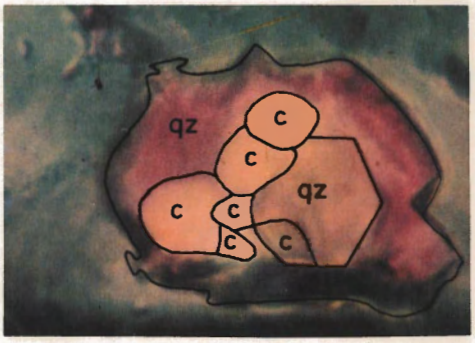


T: 173.9°C P: 27.9 MPa

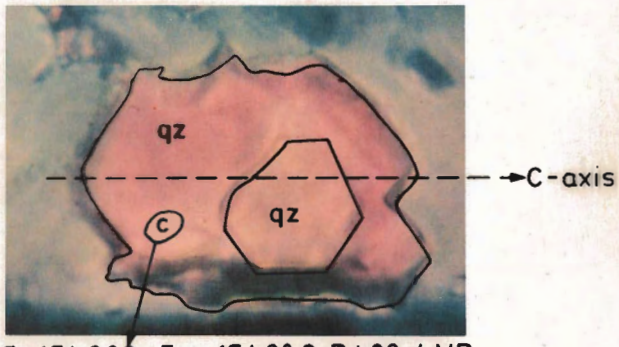


T: 174.2°C. $T_m$: 174.3°C. P: 28.4 MPa

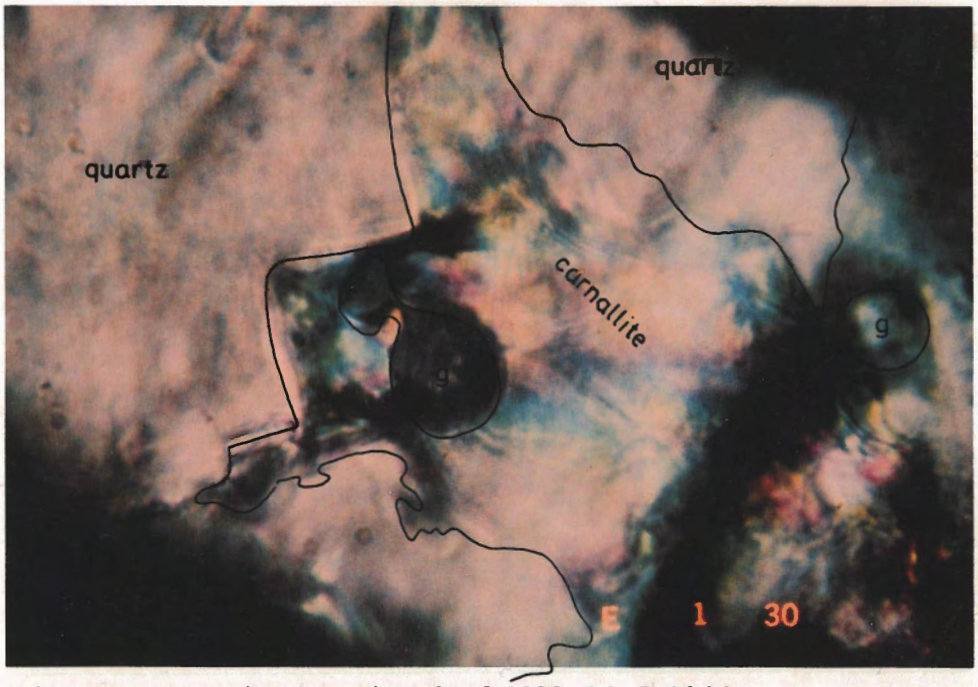


Fluid - gas - carnallite inclusion E1.30.2800. I.3. T: 20°C

PLATE I

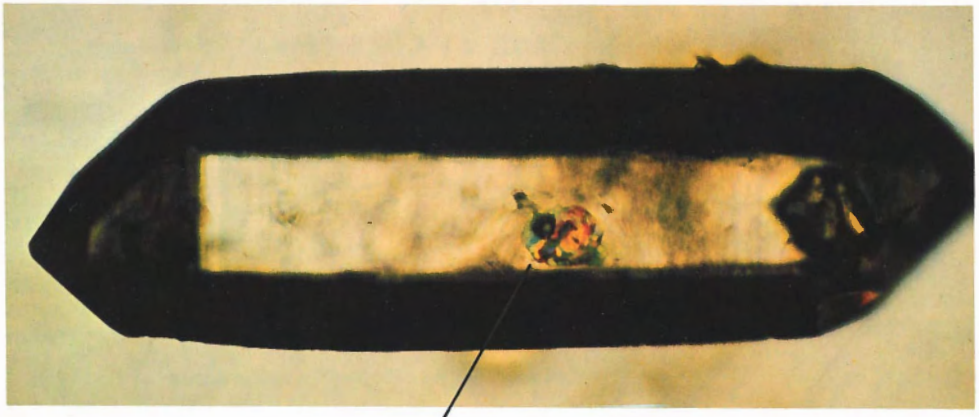

Quartz crystal E1.30.2800.IV, 945 x 270 µm, with inclusion No. 3, ø 80 µm. T: 20°C

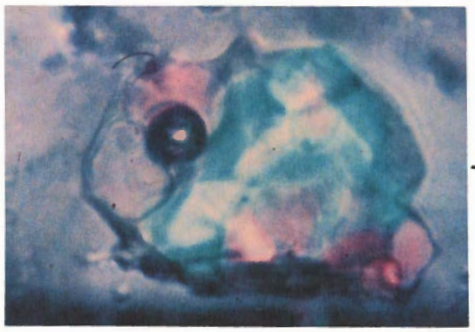

T: ~115°C. $P_{vap}$

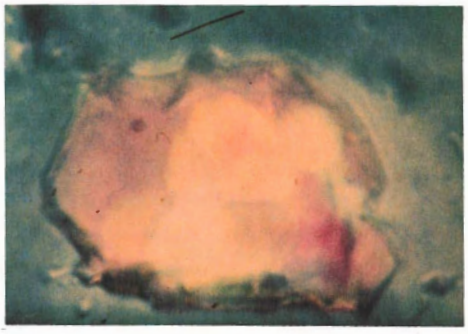

T: ~140°C. $T_h$: 147.8°C $P_{vap}$

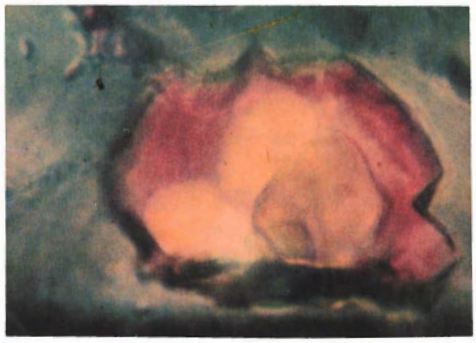

T: 173.9°C P: 27.9 MPa

T: 174.2°C. $T_m$: 174.3°C. P: 28.4 MPa

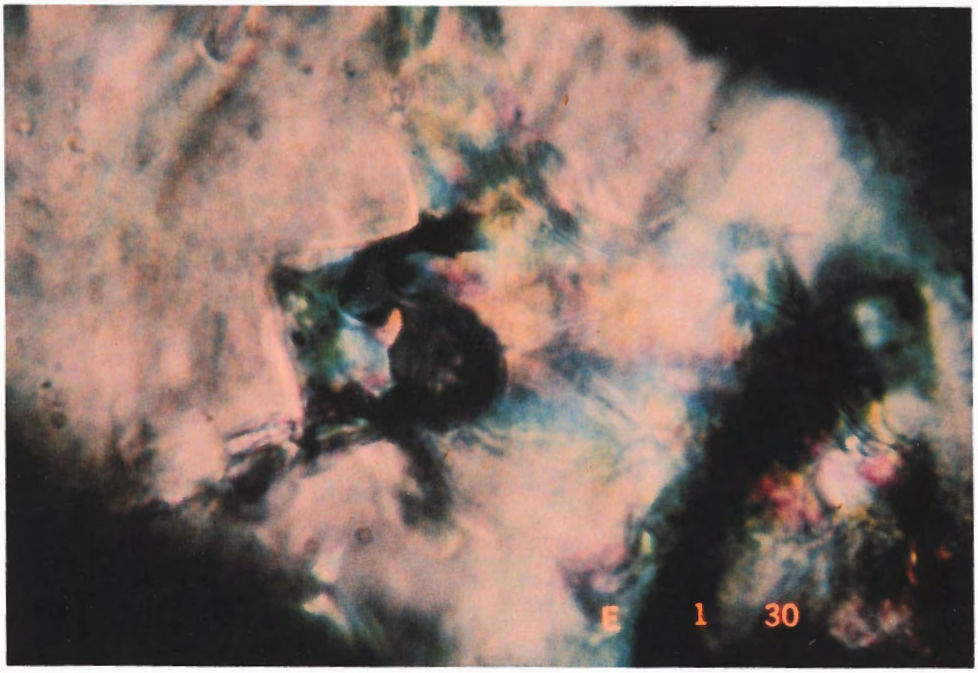


Fluid - gas - carnallite inclusion E1.30.2800. I.3. T: 20°C

# S A L T  R E S E A R C H  P R O J E C T  E F P - 8 1

Volume I. Sammendrag af Saltforskningsprojekt EFP-81. (English summary).
Editor: J.Fabricius.

Forord.

Historisk oversigt.

Kapitel 1. Stratigrafi.

Kapitel 2. Stensaltets texturelle opbygning.

Kapitel 3. Mikrotermometri.

Volume II. Stratigraphy.

Chapter 1. Lithostratigraphy of the Zechstein Salts in the Norwegian-Danish Basin.
Fritz Lyngsie Jacobsen.

Chapter 2. Description of the Oolomite-Anhydrite Transition Zone (Zechstein 1 - Zechstein 2) in the Batum-13 well, Northern Jutland, Denmark.
Martin Sønderholm.

Chapter 3. A geochemical study on Zechstein Salt and Anhydrite from the Batum-1A well.
Niels Springer.

Volume III. Fabric Analyses of Domal Rock Salt.

Chapter 1. Textural and Petrofabric Analyses of Rock Salt related to Mechanical Test Data - a quantitative Approach.
Jørgen Gutzon Larsen.

Chapter 2. Statistical Analyses of Mechanical Properties of Rock Salt.
Per Lagoni.

Volume IV. Microthermometry.

Chapter 1. Studies of Fluid Inclusions in Halite and euhedral Quartz Crystals from Salt Domes in the Norwegian-Danish Basin.
Johannes Fabricius.

Chapter 2. Formation Temperature and Chemistry of Brine Inclusions in euhedral Quartz Crystals from Permian Salt in the Danish Trough.
Johannes Fabricius.

Chapter 3. The Thermal Stability of Natural Carnallite in Cognate Geological Environments.
Johannes Fabricius.

Fluid inclusions in quartz crystals from Danish salt domes have been studied in order to determine the chemistry of the brines present in the salt.
The crystallization temperatures and the corresponding pressures of several quartz crystals have been measured and calculated. These P-T conditions reflect the diapiric evolution: pillow stage, diapiric penetration phase and post-diapiric phase. Som of the P-T measurements give strong evidence of thermal convection conditions in the bedded rock salt.
Carnallite bearing fluid inclusions have been studied in order to establish the dehydration conditions of natural carnallite in cognate geological environments. The inclusions are natural visual autoclaves and they represent a chemically closed system. Several dehydration temperatures have been measured and the corresponding pressures calculated.

Geological Survey of Denmark
Thoravej 31
DK 2400 Copenhagen
Denmark
Phone + 45 1 10 66 00

ISBN 87 88640 08 6 (bd. 1-4)